Effect of Hyperbaric Oxygen on Non-Grafted and Grafted Calvarial Critical-sized Defects

by

Ahmed MohammedSaeed Abdullah Jan

A thesis submitted in conformity with the requirements

For the degree of Master of Science

Graduate Department of Dentistry

University of Toronto

Ahmed MohammedSaeed Abdullah Jan

Effect of Hyperbaric Oxygen on Non-Grafted and Grafted Calvarial Critical-sized Defects

ABSTRACT:

Objectives:

The purpose of this study was to evaluate whether the effects of hyperbaric oxygen (HBO) therapy could alter the critical size defect (CSD) diameter and to evaluate the effect of HBO on the repair of CSD in the presence and absence of a non-vascularized autogenous bone graft (ABG).

Study Design:

Twenty rabbits were divided in two groups of ten animals each. CSD were created in the parietal bones bilaterally. Defects were critical-sized, 15 mm on one side and supracritical-sized, 18 mm on the contralateral side. Group 1 received a 90-min HBO treatment sessions at 2.4 absolute atmospheric pressure (ATA) for 90 minutes per day for 20 days. Group 2 served as a normobaric roomair control (NBO). Additional ten animals were divided into 2 groups of 5 animals each. Bilateral CSD were created. ABG were allocated to one side of each calvarium. Group 1 received HBO treatments. Group 2 served as NBO. After sacrifice, data were collected including qualitative assessment, radiographic analysis, Micro CT bone analysis and histomorphometric analysis. ANOVA and paired sample t test were used for statistical analysis.

Results:

Both radiographic analysis and histomorphometric analysis demonstrated more new bone in the HBO CSD ($p<.001$). Micro CT analysis indicated a higher bone mineral content (BMC) in ABG CSD ($p<.05$). Histologically, complete bridging of the defect was observed in ABG defects. Histomorphometric analysis showed that HBO treatment increased new bone and marrow and reduced fibrous tissue in the defects ($p<.01$ for all).

Conclusion:

Bone regeneration was significantly greater in the HBO animals regardless of the defect size. HBO may have changed the accepted diameter of CSD to more than 18 mm. HBO enhances bony healing in non-grafted CSD.

Acknowledgment

I wish to thank all the members of my research committee for their help with this project, in particular my supervisor Prof. George Sándor who was unconditionally supportive and encouraging and Prof. Cameron Clokie for his guidance with this project and tutoring over the past five years.

Thank you to Dr. Howard Holmes for the strong and positive reinforcement.

I would also like to thank Dr. Sean Peel for his continual help with statistical and analytical methods.

This work could not have been completed without the help of Dr. Amir Mhawi, Mrs. Susan Carter, Dr. Tommy Fok, Dr. Mark Bell, and Ms Anusha Rayar.

I wish to express my gratitude to my two sons, Saeed and Yousef, for their support and understanding and to my wife Fatima for her love and patience.

My two co-residents Dr. Justin Garbedian and Dr. Martin Cloutier have been true friends and more than brothers. They made this residency experience enjoyable and memorable.

I dedicate this work to my sponsor, King Abdulaziz University, Faculty of Dentistry, Jeddah, Kingdom of Saudi Arabia for giving me the opportunity of my life time.

TABLE OF CONTENTS

Chapter I: Introduction

1- Background

Maxillofacial skeletal defects result from congenital deformities, ablative surgery and trauma injuries. Reconstruction of maxillofacial defects aims at restoring form and function. Following maxillofacial trauma, vascular disruption develops in the bony skeleton which leads to the formation of a hypoxic zone. While hypoxia is necessary to stimulate angiogenesis and revascularization, extended hypoxia will blunt the healing process. Hypoxia inhibits fibroblast proliferation, collagen synthesis and granulation tissue formation (Tandara & Mustoe, 2004). Hyperbaric oxygen (HBO) involves the exposure of a patient to 100% oxygen at elevated pressures. HBO has been used as a treatment modality to improve the healing of a variety of compromised or hypoxic wounds including diabetic ulcers, radiation induced tissue damage, gangrene and necrotizing anaerobic bacterial infections (Hunt, Ellison & Sen, 2004), (Broussard, 2004), (Fenton et al., 2004).

HBO therapy is thought to aid wound healing by increasing the amount of oxygen dissolved in the blood (oxygen tension) which in turn can increase the amount of oxygen delivered to a hypoxic wound site (Shirely & Ross, 2001). HBO can promote angiogenesis (Sheikh et al., 2005) and results in an increase in the vessel density in irradiated tissue (Marx et al., 1990).

The current standard of practice for the treatment of critical-sized defects in the maxillofacial region is the use of autogenous bone grafts. While for small defects bone grafts can be obtained from intra-oral sites (Kainulainen et al., 2005), larger defects

require the harvesting of bone from extra-oral sites which require a second surgical site and result in increased risks of complications (Kainulainen et al., 2002b).

Studies have demonstrated that HBO increases bone formation in bone harvest chambers in rabbits (Nilsson et al., 1988) and elevates alkaline phosphatase activity, a marker of bone formation, in rats following mandibular osteotomy (Nilsson, 1989). HBO also results in increased osteoblastic activity and angiogenesis in irradiated mandibles undergoing distraction (Muhonen et al., 2004), (Muhonen et al., 2002c).

These results suggest that HBO may alter the critical size of calvarial defects and minimize the amount of graft required to achieve adequate bone healing of such defects. A critical-sized defect is by definition the smallest full thickness osseous wound that will not heal spontaneously during the lifetime of an animal (Schmitz & Hollinger, 1986). Such a defect requires an adjunctive technique to permit its complete bony healing. The rabbit calvarial critical-sized defect model has been used to study the efficacy of a variety of bone substitute materials in promoting defect healing (Clokie et al., 2002), (Moghadam et al., 2004). HBO has been used to aid in the healing of hypoxic or compromised wounds (Feldmeier, 2003), (Brown, Evans & Sàndor, 1998), (David et al., 2001) such as hypoperfused grafts, radiation-induced side effects (Bui et al., 2004), and necrotizing anaerobic bacterial infections (Larson et al., 2002), Fenton et al., 2004). Further, HBO have demonstrated more osteoblastic activity and osteogenic potential in rabbits' irradiated distracted mandibles when compared to a non-HBO treated group (Muhonen et al., 2004), (Muhonen et al., 2002b), (Muhonen et al., 2002a). Consequently, we hypothesized that HBO treatment would promote the healing of a rabbit critical-sized calvarial defect, possibly even allowing a supra-critical sized defect

to heal reducing the need for autogenous bone grafting. HBO therapy could therefore reduce risks, complications and possibly the cost of maxillofacial reconstruction.

2- Biology of Autogenous Bone Graft Healing

Three processes are involved in the healing of bone defects treated with bone grafts. Osteogenesis, osteoinduction and osteoconduction (Burchardt, 1983).

I.   Osteogenesis is defined as the formation of new bone from osteocompetent cells contained within a bone graft.

II. Osteoinduction is defined as bone formation from primitive mesenchymal cells in the recipient bed, which have been stimulated to differentiate into bone forming cells by inductive proteins within the graft.

III. Osteoconduction is defined as ingrowth of capillaries and osteoprogenitor cells from the recipient bed into and around the grafted material.

Through the processes of osteogenesis, osteoinduction and osteoconduction, different elements of bone tissue contribute toward the healing of grafts (Gray, Phil & Elves, 1982). Endosteum, periosteum osteocytes and marrow spaces contributes via different percentages. Gray, Phil and Elves estimated this contribution as:

1.   Endosteum 60%

2.   Periosteum 30%

3.   Osteocytes 10%

4.   Marrow 0%

Osteoblasts are immature bone cells responsible for synthesis and secretion of osteoid which is rapidly mineralized to form bone. Osteocytes are entrapped osteoblasts

responsible for the maintenance of the extracellular matrix of bone. Osteoclasts on the other hand are large multi-nucleated cells derived from macrophage-monocyte cell lines and responsible for the resorptive processes and remodeling of bone. Organic Extracellular Matrix is made of inorganic salts namely hydroxylapatite crystals and ground substance namely glycoproteins. The extracellular matrix also has a fibrous component, the most prominent of which is type I collagen.

Periosteum contains condensed fibrous tissue located on the outer surface of bone. The inner layer of the periosteum contains osteoprogenitor cells that have the capability to differentiate into osteoblasts. With the exception of the articular surfaces of bone, periosteum is bound to bone by Sharpey's fibers which exist at the sites of insertion of tendons and ligaments into bone. Periosteum plays an important role in healing of critical-sized defects (Ozerdem et al., 2003). Bone marrow contains dividing pluripotent stem cells which are located in the intertrabecular spaces of cancellous bone. Bone marrow can be active (Red marrow) or fibrofatty (Yellow marrow), which may be reactivated if the need for haemopoiesis arises.

Woven Bone is immature bone with randomly organized collagen fibers. It is much coarser than lamellar bone. Woven bone is the first version of bone to form during development and also during gap healing of bony defects if the gap is more than 0.3 mm. Woven bone continuously remodels over approximately 6 months to form lamellar bone. The time needed for transforming woven bone into lamellar bone is known as "Sigma", which is a species specific value. The Sigma for humans is 18 weeks, which explains why surgeons wait at least 4 months before applying functional loads to

autogenous bone grafts. The sigma for rabbits on the other hand, is only 6 weeks (Parfitt, 1976).

Lamellar Bone forms most of the mature skeleton. It comprises a solid mass "compact bone" and spongy mass "cancellous bone". Compact bone has a unique physical structure. Bony columns in compact bone are parallel to the axis of stress representing concentric bony layers or lamellae. Central channels contain lymphatic vessels, blood vessels, nerves and are known as Haversian canals. Volkmann's canals are also neurovascular bundles which interconnect haversian canals at right angles. As osteoblasts lay down bone peripherally, they get trapped as osteocytes in lacunae with connecting canaliculi. Cytoplasmic extensions within canaliculi connect osteocytes together and with osteoblasts as well.

The outermost layers of a bone consist of concentric lamellae of dense cortical bone while the inner layer is the medullary aspect. The medullary bone has irregular lamellae and trabeculae of spongy bone. Cancellous bone is synonymous with spongy bone. The network of irregular bony trabeculae separates the bone marrow spaces from each other. Trabeculae are lined by endosteum that is structurally similar to periosteum with osteoprogenitor cells, osteoblasts and osteoclasts. Bony lacunae contain osteocytes with canaliculi. Cancellous trabeculae have no haversian systems. Metabolite exchange occurs via canaliculi and blood sinusoids in the bone marrow.

Auxhausen described autogenous bone grafts as inert collections of transplanted bone which eventually loose their vitality and become replaced by new bone through neoangiogenesis and cell differentiation (Axhausen, 1907). This process was termed creeping substitution. Others have demonstrated *in vivo* new bone formation with

grafted autogenous bone in the muscle pouches of dogs (Ham & Gordon, 1952). The

theory that Ham and Gorlin adopted was that some cells survived within the graft and

continued to grow new bone.

A critical distance of 0.3 mm was thought to be required for surviving cells to

acquire nutrients from canaliculi at the bone surface and form lamellar bone. If the gap

was larger than 0.3 mm but up to 1 mm, then woven bone formed first and further

transformed or remodeled into lamellar bone (Schenk & Willenegger, 1977).

Many investigators described two phases of bone formation in autogenous bone

graft healing (Axhausen, 1956), (Gray & Elves, 1979), (Marx, 1993)

I) Phase I: transplanted cells within the graft formed new bone during the first

week of healing and continued for approximately four weeks. Nutrition was

acquired through diffusion from the recipient bed. The amount of new bone

formed correlated with the number of surviving transplanted cells.

II) Phase II: Bone formation began in the second week of grafting and peaked

around the fourth or fifth week. Phase II continued for life as bone

remodeling. The graft integrated during this period of remodeling.

3- Animal Model

The critical-sized defect model of the rabbit parietal bone was used in these

studies. This model has proven to be reproducible and reliable by multiple investigators

(Clokie et al., 2002), (Moghadam et al., 2004), (Haddad et al., 2006). The rabbit

calvarial critical-sized defect model provides sufficient defect volume which is

surrounded by both cortical and cancellous bone within a membranous bone. The rabbit

calvarial critical-sized defect model resembles maxillofacial bone healing. One important difference compared to other anatomical sites is the presence of a pulsatile dural layer in the base of calvarial full thickness defects, which is not present in the maxillofacial skeleton (Ozerdem et al., 2003).

A critical-sized defect is best defined as the smallest osseous wound that will not heal spontaneously during the experimental period or the life of the animal (Hollinger, Buck & Schmitz, 1994). Host systems induce healing via fibrous union in place of bone. The critical-sized defect is large enough to exceed the body's ability to regenerate bone and healing occurs by a fibrous band of tissue instead.

The quantity of bone regenerated in the critical-sized defects is influenced by the animal species, the age of the animal, the anatomic location of the defect, the size of the defect and finally the intactness of the periosteum (Schmitz & Hollinger, 1986).

Calvarial critical-sized defects receive their blood supply from the overlying pericranium and the underlying dura, unlike long bone defects, which rely on nutrient canals and intact periosteum. Intact periosteums as well as dura are also essential for bone regeneration in full thickness calvarial defects (Ozerdem, 2003).

4- Hyperbaric Oxygen Therapy

    1. Definition

Hyperbaric oxygen therapy is defined as intermittent exposure to 100% oxygen under pressures greater than 1 absolute atmosphere (ATA).

2. History of Hyperbaric Oxygen

The development of hyperbaric medicine is closely linked to the history of diving medicine. In the first documented use of hyperbaric therapy, the British physician Henshaw used compressed air for medical purposes in 1662. In 1775, Joseph Priestly was credited with having discovered oxygen. A system for treating diving accident victims using HBO was proposed by Drager in 1917, but it was not until 1937 that Behnke and Shaw used HBO to treat decompression sickness (Severinghaus, 2003).

Since the 1930s, HBO therapy has been widely used in diving medicine and for numerous other medical conditions. The accredited use of HBO is regulated by the Undersea and Hyperbaric Medicine Society which update their guidelines periodically. Unfortunately, unproven claims and speculation have made HBO's role, if any, in the treatment of some of these illnesses unclear. Tissues treated with HBO have increased levels of oxygen, which in turn have a negative effect on anaerobic bacteria (Fenton et al., 2004) and a positive effect on blood flow to the area (Marx et al., 1990). HBO has positive effects on osteoblastic activity (Muhonen et al., 2004). HBO reverses hypoxia, hypocellularity, and hypovascularity of irradiated tissues (Brown et al., 1998).

3. Physics of Hyperbaric Oxygen

In order to understand the physics of hyperbaric oxygen, one should realize that the normal pathway of oxygenation is ventilation through pulmonary alveoli followed by transport through the vascular system. There is an orderly arrangement of alveolar capillaries, the pulmonary venous system, the left atrium, the left ventricle, the systemic arterial system and tissue capillaries which finally not only bring blood and nutrients to the interstitial space but remove waste metabolites. Pressure gradients govern oxygen

8

diffusion in the interstitial space. Partial pressure of oxygen varies from arterial and venous circulations. The partial pressure of oxygen in the alveoli (PAO$_2$) equals 104 mmHg. While the partial pressure of oxygen in arterial blood (PaO$_2$) equals 90 mmHg and in the venous blood (PvO$_2$) it equals 40 mmHg. The oxyhemoglobin dissociation curve determines the dissociation of oxygen from the hemoglobin molecules as the blood components reach the tissues.

The air we breathe, which is room air, consists of 21% oxygen, 79% Nitrogen and 0.04% carbon dioxide. Air pressure at sea level equals 780 mmHg which is represented by one Absolute Atmosphere (ATA). Dalton's law calculates the total pressure exerted by a gaseous mixture as being the sum of the partial pressures of each individual component in a gaseous mixture. According to Dalton's law the partial pressure of oxygen in room air equals 160 mmHg at the sea level.

PO2= 780 X 21/100 = 160 mmHg

The pressure of gas in fluids, such as plasma for example, is calculated by Henry's Law

Gas concentration = pressure X solubility coefficient

The solubility coefficient is directly proportional to the temperature of the tissue.

4. Physiology of Hyperbaric Oxygen

Hyperbaric oxygen therapy is defined as intermittent exposure to 100% oxygen under pressures greater than 1 absolute atmosphere (ATA). The concentration of oxygen in the atmosphere is 21%. At 1 ATA, the oxygen in blood is almost entirely carried by hemoglobin. While 97% of oxygen carried in the arterial blood is chemically bound to haemoglobin while only 3% is dissolved in plasma. One gram of haemoglobin

carries a maximum of 1.34 ml of oxygen. Fully saturated haemoglobin (100%) in 100ml of blood carries approximately 20 ml of oxygen, while 97% saturated haemoglobin in 100 ml of blood carries 19.5 ml of oxygen. The 19.5 ml amount is reduced to 5ml of oxygen while blood passes through the capillaries. Increasing the oxygen-carrying capacity of blood by increasing hemoglobin saturation is not possible.

At sea level, the gas pressure is 760 mmHg or 1 Atmosphere Absolute (ATA) and arterial haemoglobin saturation is 97%, while venous haemoglobin saturation is 70%. Inhalation of HBO increases the quantity of oxygen dissolved in plasma. At 1 ATA, the amount of dissolved oxygen in 100 ml of plasma is 0.449 ml. When inhaling 100% oxygen at 1 ATA, the O_2 concentration increases to 1.5ml / 100 ml of plasma. When inhaling 100% oxygen at 3 ATA, the amount of dissolved oxygen in 100 ml of plasma increases to 6.422 ml / 100 ml of plasma, which is enough to meet the basic metabolic needs of healing tissues in the human body (Marx et al., 1990).

The driving force for oxygen diffusion from the capillaries to tissues can be estimated by the difference between the partial pressure of oxygen on the arterial side and the venous side of the capillaries. The difference in the partial pressure of oxygen from the arterial side to the venous side of the capillary system is approximately 37 times greater when breathing 100% oxygen at 3 ATA than room air at 1 ATA. The distance which oxygen can diffuse is 15 to 20 times greater in tissues exposed to HBO.

Improving abnormally low tissue oxygen concentrations has been shown to accelerate healing (Conconi et al., 2003). Fibroblast synthesis of collagen requires tissue oxygen tensions of 30-40 mm Hg. HBO therapy has the potential to achieve these levels in hypoxic or poorly perfused tissues. *In vitro* studies have shown that

exposure to HBO for 30-minute and 60-minute periods at 2.5 ATA enhances fibroblast cell growth (Marx et al., 1990). On the other hand, 120-minute exposure to HBO at 2.5 ATA exerts a marked proapoptotic effect on fibroblasts (Conconi et al., 2003).

5. Indications of Hyperbaric Oxygen

The undersea and hyperbaric medicine society (UHMS) has approved the following medical indications for HBO therapy (Broussard, 2004):

1. Air or gas embolism

2. Carbon monoxide poisoning with or without Cyanide poisoning

3. Clostridial myositis and myonecrosis (gas gangrene)

4. Crush injury and compartment syndrome

5. Decompression sickness

6. Enhancement of healing in problem wounds

7. Exceptional blood loss (anemia)

8. Intracranial abscess

9. Necrotizing soft tissue infections

10. Refractory osteomyelitis

11. Radiation induced necrosis

12. Compromised skin grafts and flaps

13. Thermal burns

Hyperbaric oxygen (HBO) has been used to aid in the healing of hypoxic or compromised wounds (Feldmeier, 2003), (Brown et al., 1998), (David et al., 2001) such as hypoperfused grafts, radiation-induced side effects (Bui et al., 2004) and necrotizing anaerobic bacterial infections (Larson et al., 2002). Hyperbaric oxygen therapy has proven to stimulate osteoblastic proliferation and differentiation *in vitro* (Wu et al., 2007). Oxygen content in the tissues can be boosted to 81% ±5% of normal tissue after 20 sessions of HBO (Marx, 1984). Marx and Ehler have shown 9 fold increases in neoangiogenesis with HBO therapy at 2.4 ATA for 90 minutes a day for 20 days (Marx et al., 1990).

Radiation Induced Side Effects

Osteoradionecrosis (ORN) is defined as the presence of necrotic soft tissue and bone that fail to heal spontaneously and do not respond to local care over a period of 6 months (Marx, 1984). Osteoradionecrosis of the jaws is more prevalent in the mandible than in the maxilla. The richer blood supply of the maxilla partially accounts for this difference. In the mandible, the bone density is increased and there is more compact bone. The mandible also usually receives a greater dose of radiation than the maxilla during the curative treatment of cancer using radiotherapy aimed at the base of the tongue and the hypopharynx (Johnson, 1997). Risk factors such a higher body mass index, the use of steroids and radiation dose greater than 6600 Gray were found to be associated with a significant increase in ORN (Goldwaser et al., 2007).

One of the most widely accepted and extensively documented indications for HBO therapy is its application in the treatment and prevention of Osteoradionecrosis

(ORN) of the mandible. Marx developed the (Wilfred-Hall) staging Algorithm for classifying and treatment of mandibular ORN and for prophylaxis prior to tooth extraction in irradiated mandibles thought to be at risk (Marx, Johnson & Kline, 1985).

Existing Stage I ORN/ or Prior to Tooth Extraction

Exposed bone without other signs and symptoms. These patients are treated with 30 HBO therapy sessions with no debridement or only minor bony debridement. If the patient's ORN progresses, then 10 additional HBO_2 treatments are given.

Stage II ORN

Non resolving Stage I ORN. These patients are treated with 30 HBO therapy sessions followed by surgical debridement and 10 post-operative HBO therapy sessions. Debridement for Stage II ORN ideally maintains mandibular continuity.

Stage III ORN

Non resolving stage I or II and/or the mandibular continuity cannot be maintained. These patients are treated by a reconstruction protocol. Thirty HBO therapy sessions are instituted followed by mandibular resection eradicating all necrotic bone and then 10 post-resection HBO therapy sessions. Reconstruction follows in a delayed fashion. The number of HBO sessions varies according to the severity of the condition.

Although there has been controversy regarding the usefulness and the application of hyperbaric medicine as an adjunct to bone healing (Keller et al., 1997), (Wagner, Esser & Ostkamp, 1998), laboratory data has always been convincing (Marx et al., 1990). HBO therapy demonstrated an elevation of alkaline phosphatase levels in cells derived from alveolar bone (Marx et al., 1990). Similar results were also obtained from cells derived from irradiated mandibles (Muhonen et al., 2002a), (Muhonen et al.,

2004). Microangiographic studies have shown a statistically significant increase in vascular density of HBO treated irradiated mandibles when compared to normobaric 100% oxygen and normobaric room air (Marx et al., 1990).

Hyperoxia is not without complications or side effects. It causes an initial rapid and significant vasoconstrictive effect. (van Golde et al., 1999). Breathing 100% oxygen at 3 ATM leads to a reduction in perfusion of up to 25% in the brain. This may lead to neurotoxic activities manifested as convulsions in 10% of the population (Gelfand, Lambertsen & Clark, 2006). Reduction in perfusion also occurs in other tissues, although to a lesser extent. Tracheal irritation has been reported as well as burning sensation on inspiration after 6 hours of hyperoxia. This irritation may progress to severe chest pain and dyspnea (Hendricks et al., 1977). Changes in visual acuity have also been reported with HBO therapy (Gelfand et al., 2006). Administering HBO at 3 ATA for more than 1 hour results in side effects in 10% of the population. Reducing ATA to 2.5 is associated with non significant side effects. At 2 ATA, oxygen toxicity is unlikely to be evident within less than 3 hours of HBO exposure; whereas at 6 ATA, this window is reduced to a few minutes. Several hyperbaric protocols had been employed in laboratory and clinical trials. The desirable range of pressure between 2 and 2.5 ATA for 90 to 120 minutes proved to be effective with minimal if any side effects (Brown et al., 1998), (Muhonen et al., 2002a).

6. **Methods of HBO therapy Administration**

HBO can be administered using an HBO chamber by two methods. Either a single person mono-person chamber (Figure 1) or multiplace chamber (Figure 2) can be utilized. Mono-place chambers contain compressed oxygen and are designed to treat

individual patients one at a time. This method is less expensive than a multiplace

chamber. The disadvantage is limited access to patients. Conversely, multi-place

chambers contain compressed room air not compressed oxygen. Patients breath 100%

compressed oxygen through hoods or masks while sitting in the chamber. Multiple

patients can be treated in same chamber simultaneously. A trained attendant

continuously monitors the patients in the chamber. Although this method is more

expensive and needs a full time trained attendant, it is more cost effective and can

accommodate up to six individual at a time, according to the size of the chamber.

Hyperbaric oxygen therapy is costly. In the United States, Medicare pays

approximately 400 US dollars per dive for facilities fee and 125 US dollars professional

fee, resulting in an expense of 80,000 dollars for a course of 40 treatments (Attinger et

al., 2008). The potential cost of a prolonged course of HBO therapy must be weighed

against savings that may be achieved from improved tissue healing and reduction of

amputations and complicated outcomes. Facilities are often scarce. In 1996, 259

hyperbaric facilities were reported to exist in the United States. Only eleven were

reported in Canada. Accredited facilities are available only in larger cities with medical

centers or academic health science centers.

Chapter II: Aim, Objectives and Hypotheses

1- Aim

The aim of this study was to determine whether the use of HBO in the absence of a bone graft produces critical-sized defect healing equivalent to that which occurs with a bone graft and whether HBO enhances the healing of critical-sized defects which do contain autogenous bone grafts.

2- Objectives

1. To perform a gross clinical examination of critical-sized defects at 6 and 12 weeks with and without HBO therapy and at 6 weeks in the presence or absence of autogenous bone grafting.

2. To evaluate the radiographic and histologic nature of the critical-sized defects in the study groups.

3. To perform histomorphometric analysis of new bone formation in critical-sized defects.

4. To compare of new bone formation in the study groups.

5. To analyze the bone mineral content and bone mineral density in the autogenous bone graft groups.

6. To compare the bone mineral density and bone mineral content of the autogenous bone grafts treated with and without hyperbaric oxygen.

3- Hypotheses

Null Hypothesis (H$_0$)

1. HBO therapy does not affect the critical size of calvarial defects

2. HBO therapy does not affect the quality of bone formation measured by bone mineral content and bone mineral density in critical-sized defects

3. HBO therapy does not affect the amount of bone formed in critical-sized defects in the presence of autogenous bone grafting.

Alternate Hypothesis (H$_1$)

a) HBO therapy increases the critical-size of calvarial defects.

b) HBO therapy will allow bony healing of critical-sized and supra-critical-sized cranial vault defects similar to the findings with autogenous bone grafts.

c) HBO therapy will ameliorate the amount of bone generated within critical-sized defects.

Chapter III: Materials and Methods

***Phase I:** Hyperbaric oxygen results in an increase in rabbit calvarial critical sized defects.*

1. Experimental Design

Twenty adult, skeletally mature, male New Zealand White rabbits weighing 3 to 4 kg were randomly divided into 2 groups of 10 animals. Group 1 was treated with HBO, while group 2 served as a control and did not receive any supplemental oxygen. Five animals from each group were sacrificed at 6 and 12 weeks.

2. Surgical procedures

The surgical procedure was performed in a sterile fashion in accordance with the University of Toronto animal research committee protocol number 20005155. The surgical technique and the analgesic protocols have been previously described (Clokie et al., 2002), (Moghadam et al., 2004). General anesthetic was induced using intramuscular Ketamine 50 mg/kg. Monitoring involved pulse oximetry, which measures oxygen saturation and heart rate. The animals were placed in the prone position while a laryngeal mask airway was inserted into the hypopharynx just posterior to the tongue to maintain the airway. General anesthesia was maintained by a 1.5% enflurane and oxygen mixture with spontaneous ventilation. End tidal carbon dioxide levels were also monitored by a capnograph which measured respiratory rate as well.

The scalp was shaved and cleaned with betadine (Povidone-Iodine topical antiseptic solution). The animal was then prepped and draped in a sterile fashion (Figure 3). At the beginning of the procedure, approximately 1cc of 2% lidocaine with 1:100,000

epinephrine was infiltrated subcutaneously along the sagittal midline of the scalp where the planned incision line was located. Subperiosteal infiltrations followed into the parasagittal areas where the parietal bones are and where the osteotomy was planned. After allowing a few minutes for the local anesthetic and vasoconstriction to take effect, a full thickness 5 cm incision was made through skin, subcutaneous tissue, galea apponeurotica, loose areolar connective tissue and pericranium. The incision extended in the sagittal midline from the frontonasal suture back to the occipital protuberance. A subgaleal plane of dissection was developed and subperiosteal dissection followed using a series of periosteal elevators. The superior temporal ridge was exposed, which is the lateral boundary of the parietal bone. Care was taken to preserve the intactness of the pericranium. A self retaining retractor was used to retract the full thickness flap. Using a 702 fissure bur on an electrical handpiece, a full thickness osseous defect was then created in the parietal bones bilaterally under copious amounts of normal saline irrigation. Each animal had bilateral full thickness calvarial defects created in its parietal bones. Defects were allocated randomly as critical-sized, 15 mm on one side and a supracritical-sized, 18 mm on the contralateral side (Fig. 1). Standardization of defects was accomplished by using a trimmed template of the desired circumference. The osteotomy line was always kept within 2 mm from the midline sagittal suture to avoid endangering the sagittal venous sinus and to serve as a landmark for future micro CT analysis and histomorphometrics. Sharp bony edges were trimmed and the dural layer was closely examined for tears and lacerations. No clinically significant dural tears were noted during any of the surgical procedures in any of the animals. The osseous wounds were thoroughly irrigated by normal saline. The soft tissues were sutured in layers. The

Pericranium was sutured back along with the galea apponeurotica by 3-0 vicryl continuous suture and the skin was closed by the same sized suture in continuous locking fashion to insure water tight closure (Figure 3). The animal was then allowed to breathe 100% oxygen for approximately 15 minutes. The laryngeal mask airway was removed. A single dose of intramuscular injection of Bupremorphine 0.02 mg/kg was given before transferring the animal back to the husbandry area. No further analgesics were required thereafter. Since the procedure was done under sterile technique, no antibiotics were given either. Animals were individually caged and provided with water and appropriate nutrition throughout the experimental period. All animals continued to thrive throughout the experimental period.

3. HBO sessions

The 20 animals in group one (n = 10) underwent a 90-minute HBO session at 2.4 absolute atmospheric pressure (ATA) per day 5 days a week for 4 weeks (20 days total). Pressurization and depressurization were done at a very slow rate of 0.2 ATA per minute in order to avoid barotrauma and potential discomfort. The control group, group 2 (n = 10) had no HBO sessions, breathing normobaric oxygen (NBO), otherwise referred to as ambient pressure room air, during the entire experimental period. HBO treatment sessions were begun 24 hours postoperatively in a monoplace chamber specially designed for small animal use. The test group was acclimatized to the HBO chamber one week preoperatively. This involved the animals being placed in the unpressurized hyperbaric chamber breathing normal room air for 90 minutes per day for 5 days. The chamber had a glass window in its rear end allowing the investigator to monitor the rabbits' behavior and comfort throughout the 90-minute sessions (Figure 4).

4. Sacrifice and qualitative evaluation

Five animals from each group were sacrificed 6 weeks postoperatively and 5 from each group were sacrificed 12 weeks postoperatively. They were premedicated with Ketamine 50 mg/kg followed by the insertion of an intravenous line in the marginal ear vein. A standardized T-61 euthanizing agent was given as an IV push according to the subject's weight. A midline sagittal incision was made through skin and subcutaneous connective tissue exposing galea apponeurotica over the whole calvaria. The parietal region was identified. Bilateral parietal bones were harvested in a single specimen using an oscillating saw while preserving the pericranium over the defects. Care was also taken to preserve the sagittal, coronal and the lambdoid sutures because they served as references to the circumference of defects. The final harvested specimens measured 30x25x12 mm in the greatest dimensions. The specimens were examined grossly for signs of inflammation, transilluminated with incandescent light and photographed. Plain Radiography followed.

5. Plain Radiography

Radiographs of the specimens were taken using a cephalostat machine standardized for 1:1 magnification on a D speed film at 9mA, 60 KVP for 0.2 seconds. The films were processed in an automatic developer and examined for radiopacities, which represented new bone formation. Fixation followed in 10% formalin for 48 hours. Specimen containers were labeled with a separate coding to allow for blinded radiomorphometrics and histomorphometrics.

6. Radiomorphometrics

Radiographs were digitized. An investigator blinded to the HBO status of the animals traced the areas of radiopacities within the defects. The percentages of radiopacities were calculated via Image Pro Plus 4.1 software for Windows (Media Cybernetics, Carlsbad, CA).

7. Histological evaluation

Upon completion of the fixation period, decalcification followed using 45% formic acid and 20% sodium citrate for 4 weeks. Testing for adequate decalcification was accomplished by attempting to cut through a contingency intact specimen with a number 10 scalpel. Adequate decalcification was achieved in 4 weeks in all of the specimens. Each specimen was sectioned into two portions: an anterior and posterior portion. Each half was washed in distilled water for 10 minutes three times. Dehydration was accomplished by using a series of alcohol immersions starting with 70% ethanol for 15 minutes twice followed by 95% ethanol for 15 minutes twice followed by 100% ethanol for 30 minutes twice. Each specimen was then immersed in methylbenzoate overnight. Immersion in Toluene followed for 30 minutes. Specimens were then infiltrated with paraffin embedded under vacuum pressure. Paraffin blocks were then sectioned into 7µm sections, prepared and stained with hematoxylin and eosin. Sections in the middle of the defects, representing the greatest dimension (15 mm or 18 mm) were examined under the light microscope by a blinded investigator in an attempt to prevent bias.

8. Histomorphometrics

Ten sections within the middle of the each of the defects were digitized. Digital images were captured by a CCD digital camera (RT Color; Diagnostic Instruments Inc., Sterling Heights, MI) attached to the microscope on 4X magnification with 100% zoom to ensure proper focus. To create a single image from each slide the digital images were merged using Adobe Photoshop Elements 2.0 (Adobe Systems Inc., San Jose, CA). The repair tissue in each defect was measured by a blinded investigator in an attempt to prevent bias. The amount of new bone was extracted and expressed as the percentage of the total area of the defect. Calibration was achieved using a millimeter grid.

9. Statistical Analysis

ANOVA and paired sample t tests were applied in SPSS 10.0 for Windows (SPSS Inc., Chicago, IL), and used to calculate statistical differences between the means of new bone formation based on histomorphometrics. Means of the radiopacities within the defects were also analyzed. The percentage of new bone and the percentage of radiopacities were analyzed in relation to either (1) inspired oxygen (HBO vs. NBO), (2) defect size (15 mm vs. 18 mm), or (3) healing time (6 weeks vs. 12 weeks). The p values below .05 were considered to be statistically significant.

Phase II: *Effect of hyperbaric oxygen on grafted and nongrafted calvarial critical-sized defects.*

1. Experimental Design

Ten adult, skeletally mature, male New Zealand White rabbits weighing 3 to 4 kg were randomly divided into 2 groups of five animals. The animals of Group 1 (HBO) underwent HBO treatment. Rabbits were placed in a hyperbaric chamber and exposed to 100% oxygen at 2.4 atmospheres absolute for 90 minutes per day for 5 days a week for 4 weeks (20 days total). The animals of Group 2 served as normobaric controls (NBO) and were left to heal at room air without any further intervention.

Prior to the HBO treatment sessions, bilateral 15 mm full thickness osseous defects were created surgically in the parietal bones of all the animals. The surgical procedures were performed in sterile fashion in accordance with the University of Toronto animal research committee protocol number 20005155 following the same protocol described in phase I. Autogenous bone grafts were placed randomly on the right or left side of each animal. The other defect was left Non-Grafted. HBO treatment was initiated 24 hours after surgery. Animals were sacrificed 6 weeks postoperatively. The parietal bones were harvested bilaterally from each subject. Specimens were examined grossly, fixed, scanned by micro-computed tomography. Histological examination was followed by histomorphometry.

2. Surgery

The surgical procedure was performed in sterile fashion in accordance with the University of Toronto animal research committee protocol number 20005155. The same protocol in phase I was followed in terms of general anesthetic, airway maintenance, monitoring and surgical access (Figure 5). Bilateral full thickness osseous defects were created. In phase II, defects measured 15 mm in the smallest dimension. Standardization of the defects was accomplished by using a sterile trimmed foil template of the desired circumference. The resultant two blocks of calvarial bone were particulated by a double action rongeur forceps and stored in a chilled normal saline container. Clinically insignificant dural tears were noted in few animals. The osseous wounds were thoroughly irrigated by normal saline. Autogenous corticocancellous chips were then packed into one of the defects and the contralateral defect was left void to fill in with a blood clot. Wound closure and postoperative care followed the same protocol as in phase I.

1. Hyperbaric Oxygen Therapy (HBO)

The same HBO protocol was followed for phase II as in phase I.

2. Sacrifice and qualitative evaluation

All rabbits were sacrificed six weeks postoperatively. The same protocol was followed. The difference in phase II was the plan to perform bone analysis through micro-computed tomography scans. Hence, the specimens were fixed for only 48 hours then scanned and fixed for an additional 24 hours before proceeding to histological preparation.

3. Plain Radiography

Radiographs of the specimens were taken using a cephalostat machine standardized using the same specifications used for phase I study. Radiopacities within defect may represent either new bone formation or the autogenous bone graft. Fixation followed in 10% formalin for 48 hours. Specimen containers were labeled with a separate coding to allow for blinded micro CT analysis and histomorphometrics.

4. Micro-Computed Tomography

48 hours after fixation, micro computed tomography (mCT) followed. This study utilized an Explore Locus SP® micro CT scanner (GE medical systems, London, Ontario, Canada). This scanner was designed to scan specimens that measure at most 25 x 30 mm, which corresponds to a bilateral parietal bone specimen containing both defects. It was impractical to scan the entire calvarium. Prior to scanning the specimens, a calibration scan was performed using a synthetic bone sample, a water sample and an air sample. Calvarial specimens were scanned using the fast mode utilizing 0.05mm sections. Each specimen took 120 minutes to be fully scanned. Reconstruction of scanned images (Figure 6) was done using Microview software (GE Medical Systems, London, Ontario, Canada) after calibrating the program using the bone, water and air standard values. The reconstructed 3D image was then traced in 3 dimensions to the circumference of the original defect margins. This allowed the creation of a 3D reconstruction of the defect, which was referred to as the region of interest (ROI)

5. Bone Analysis

A reconstructed intact specimen was used to set up the bone value threshold, which was analyzed by the same software. A normal distribution curve had determined the bone value threshold to be at 1300 at a 95% confidence interval. The bone value was used to differentiate bone from non-bone tissues within the defect and to guide the software in measuring tissue mineral content. The region of interest was analyzed using the following parameters:

1- Total Defect Volume (TV) in (mm^3)

2- Bone Volume (BV) in (mm^3): Tissues that matched bone value threshold of 1300 at 95% confidence interval.

3- Bone Volume Fraction (BVF): Percentage of bone volume by total defect volume (BV/TV)

4- Bone mineral content (BMC) mg/mm^3): Measurement of bone mass in the organic matrix.

5- Bone Mineral Density (BMD): Percentage of bone mineral content in the total defect volume.

6- Tissue Mineral Content (TMC) in (mg/mm^3): bone mineral content of voxels within the ROI.

7- Tissue Mineral Density (TMD): Percentage of tissue mineral content in the total defect volume.

8- Histological Preparation

Upon completion of micro CT scanning, the specimens were put in the fixative for additional 24 hours. Histological preparation followed using the same protocol utilized in phase I study.

9- Histomorphometry:

Ten sections within the middle of the defects were digitized and analyzed using the same methods and instruments. Since one side of the calvaria was grafted with autogenous bone, a blinded investigator traced the images for new bone formation as well as bone marrow, fibrous tissue and residual bone graft. Values were extracted and calculated as percentages in the total area of the defect.

10-Statistical Analysis:

All data was tested for normality and equal variance. Results were compared across all groups using 1 and 2 way ANOVA with Student Newman Keuls (SNK) post hoc testing for normal data of equal variance or Holm-Sidak post hoc testing for non-normal/non equal variance data. Paired t-tests were used to compare the defects within the animals. As there was bone graft in only 2 groups, a t-test was used to compare the amount of residual graft between the HBO and NBO defects which had been grafted with autogenous bone. All statistical analyses were performed using SigmaStat v3.5 (Systat Software San Jose CA). Statistical significance was considered to be at $p<.05$.

Chapter IV: Results

Phase I: *Hyperbaric oxygen results in an increase in rabbit calvarial critical sized defects.*

I. **Qualitative Evaluation**

    a. **Normobaric Room Air Oxygen (NBO) Group**
        i. Clinical Findings on Gross Examination

Defects were uniformly occupied by a thin membrane of flexible tissue. No dehiscence was noted. The junction between this thin flexible membrane and the native bone was clearly demarcated by palpation. The dural and the pericranial layers were intact. Appreciable difference was noted in the size of the 15 and 18 mm defects as expected

        ii. Radiographic Findings (Figure 7)

The radiographs of the NBO defects showed a well demarcated radiolucency with noncorticated borders. Very small areas of radiopacities were often seen within 2 mm from the defect margin, which indicated modest bone formation within 1-2 mm of the defect margin. No difference was grossly noted between the critical and the supracritical sized defects

        iii. Histological Findings (Figure 8)

NBO defects were predominantly filled with fibrous tissue that contained an occasional blood vessel. Defect margins were readily identified. New bone was mostly restricted to the defect margins although small islands of woven bone were occasionally seen in the fibrous tissue more centrally.

b. Hyperbaric Oxygen Treated (HBO) Group:

i. *Clinical Findings*

The HBO defects were occupied by firmer tissues that resemble the hardness of bone. The junction between native bone and the defect contents were not palpable. The dural and the pericranial layers demonstrated similar appearances as the NBO counterparts

ii. *Radiographic Findings (Figure 7)*

Islands of radiopacities were noted around the defect margin extending more than 5 mm toward the center of the defect in the 6 week samples, while in the 12 week samples, radiopacities almost approached the center of the defect. These islands presented with variable densities. Defect margins were still identifiable.

iii. *Histological Findings (Figure 8)*

The HBO defects were completely bridged with bony tissue. This bridge consisted of newly formed cortical bone with vascular marrow. Defect margins were readily identified.

II. Quantitative Evaluation

a. Radiomorphometrics (Table 1)

Radiomorphometric findings are presented in table 1 and graphically shown in figure 9. More islands of radiopacities in the HBO group compared to the control group in both the 6- and 12-week specimens ($p<.001$). There were fewer radiopaque foci within the margins of the defects in the control group. In the control group the radiopacities tended to blend with the margins of the defects, whereas in the HBO group more radiopaque areas were evident both along the margins as well as in the center of the defects (Figure 7). No differences were noted between the 15-mm and 18-mm defects ($p=.688$).

The percentage of radiopacities were greater in HBO samples at 12 weeks when compared to those at 6 weeks (p=.019).

Table 1: Percentages of radiopacities at 6 and 12 weeks of Critical-sized (15 mm) and Supracritical-sized (18 mm) defects

Sacrifice time	6 WEEKS				12 WEEKS			
Defect size	15 mm		18 mm		15 mm		18 mm	
Oxygen	HBO	NBO	HBO	NBO	HBO	NBO	HBO	NBO
Percent radiopacities within defects	52.96	38.31	29.73	29.86	79.51	47.29	95.50	20.39
	27.92	29.46	61.34	41.22	65.41	30.85	76.97	23.16
	60.18	45.72	65.25	43.67	95.13	2.10	92.24	39.02
	57.85	47.39	44.22	26.60	90.35	30.50	98.74	54.07
	44.98	35.84	51.55	29.62	67.03	54.67	74.94	65.88
Mean	48.78	39.34	34.19	50.42	79.49	33.08	87.68	40.50
SD	13.03	7.35	14.20	7.69	13.38	20.24	10.97	19.59
SE	5.83	3.29	6.35	3.44	5.98	9.05	4.90	8.76

b. Histomorphometrics (Table 2)

Histomorphometric findings are presented in table 2 and graphically shown in figure 10. Histomorphometric analysis demonstrated more bone formation in the HBO group when compared to the control group ($p<.001$). Both critical sized (15 mm) and supracritical sized (18-mm) defects healed with significantly more bone in the HBO group when compared with the control group. There was no significant difference between the percentage of new bone formed in the 15 mm and the 18 mm defects ($p=.520$), nor between the 6-week and 12-week groups ($p=.309$).

Table 2: Percentages of new bone formation at 6 and 12 weeks of Critical-sized (15 mm) and Supracritical-sized (18 mm) defects

Sacrifice time	6 WEEKS				12 WEEKS			
Defect size	15 mm		18 mm		15 mm		18 mm	
Oxygen	HBO	NBO	HBO	NBO	HBO	NBO	HBO	NBO
Percent new bone formation	64.22	20.63	74.89	30.23	64.02	18.68	58.56	6.84
	49.60	22.77	43.36	45.33	58.06	10.07	52.58	20.03
	67.22	33.26	75.77	46.55	46.67	14.53	57.35	19.90
	53.94	22.64	49.34	24.48	55.39	10.02	50.46	24.16
	47.73	20.01	61.04	22.75	56.67	17.61	39.25	42.26
Mean	56.54	23.86	60.88	33.87	56.16	21.46	51.64	26.83
SD	8.74	5.31	14.65	11.37	6.25	18.20	7.67	15.36
SE	3.91	2.41	6.55	5.08	2.80	7.43	3.44	6.27

Phase II: _Effect of hyperbaric oxygen on grafted and nongrafted calvarial critical-sized defects._

I. **Qualitative Evaluation**

a. **Normobaric Room Air Oxygen (NBO) Group (Figure 11)**

   i. *Non-Grafted Defects:*
      1. *Clinical Findings*

 The Non-Grafted defects were uniformly occupied by a thin membrane of flexible tissue. No dehiscence was noted. The junction between this thin flexible membrane and the native bone was clearly demarcated by palpation. The dural and the pericranial layers were intact.

      2. *Radiographic Findings*

The radiographs of the Non-Grafted defects showed a well demarcated radiolucency with noncorticated borders. Very small areas of radiopacities were often seen within 2 mm from the defect margin, which indicated modest bone formation within 1-2 mm of the defect margin

      3. *Histological Findings*

The Non-Grafted NBO defects were predominantly filled with fibrous tissue that contained an occasional blood vessel. Defect margins were readily identified. New bone was mostly restricted to the defect margins although small islands of woven bone were occasionally seen in the fibrous tissue more centrally (Figure 12).

ii. Autogenous Bone Grafted Defects:
1. Clinical Findings

The grafted NBO defects were uniformly occupied by firmer tissues that resembled the hardness of bone. The junction between native bone and the defect contents were not palpable. The dural and the pericranial layers demonstrated similar appearances as the Non-Grafted counterparts

2. Radiographic Findings

Particles of autogenous bone were clearly visualized within the defects with variable densities. Defects margins were still identifiable.

3. Histological Findings

The grafted NBO defects were completely bridged with bony tissue. This bridge was a mixture of non-vital cortical bone from the graft, newly formed bone and vascular marrow (Figure 13). Defect margins were readily identified.

b. Hyperbaric Oxygen Treated (HBO) Group (Figure 14)

i. Non-Grafted Defects:
1. Clinical Findings

The Non-Grafted HBO defects demonstrated similar gross morphological features to their Non-Grafted NBO counterparts

2. Radiographic Findings

Defects were occupied with a homogeneous radiopaque shadow. This shadow was denser than what appeared in the NBO Non-Grafted defects but still less dense than the grafted defects. Margins of the defects were poorly demarcated.

3. Histological Findings

It was difficult to distinguish the defect margin in the Non-Grafted HBO treated defects.

The defects were completely bridged with new bone, which tended to thin towards the

centre of the defects, with the dural and periosteal edges being composed of denser

fibrous tissue. The new bone contained marrow elements which were not as extensive

as in the grafted defects (Figure 15).

ii. Autogenous Bone Grafted Defects:

1. Clinical Findings

The grafted HBO defect demonstrated similar gross morphological features to their

Grafted NBO counterparts

2. Radiographic Findings

Defects appeared to be homogenously radiopaque with less demarcated defect

borders. Bone graft particles were blended together and less recognizable with more

homogenous radiopacity.

3. Histological Findings

Margins of the defect were difficult to identify in the grafted HBO treated defects.

These defects were completely bridged with extensive amounts of new bone and

marrow. Minimal devitalized remnants of the graft were still visible (Figure 16).

2- Quantitative Micro-Computed Tomography (Table 3)

Statistical analysis of the micro CT results are presented in table 3 and graphically illustrated in figure 17, 18, and 19. They indicated that the presence of the graft resulted in increased BV, BMC, BMD and BVF compared to Non-Grafted defects under both NBO and HBO ($p<.05$). Comparisons between the HBO and NBO autogenous bone grafted defects revealed that the HBO grafted defects had significantly lower BV ($p=0.03$) and BMC ($p<.05$). However, the reductions in BVF and BMD did not reach significance ($p=0.123$ and 0.078 respectively). No significant differences between the HBO and NBO Non-Grafted defects were seen in any of the parameters measured.

Table 3: Micro CT analysis is demonstrated among the study groups and statistically analyzed using 1-Way ANOVA

	NBO		HBO		1-Way ANOVA
	Non-Grafted	ABG	Non-Grafted	ABG	p value between groups
TV(mm^3)	233±37	263±55	191±27	189±66	0.076
BV(mm^3)	41±7	140±22	39±17	87±36	<0.001
BVF (%)	17.6±2.1	53.9±6.4	20.0±7.3	46.2±11.0	<0.001
BMC (mg)	31.2±6.3	118.0±21.3	32.4±13.0	76.0±27.6	0.002[a]
BMD (mg/mm^3)	134±20	451±25	167±53	403±52	<0.001
TMC (mg)	25.6±4.5	90.3±13.5	23.8±11.3	53.9±24.1	<0.001
TMD (mg/ mm^3)	627±27	645±20	602±26	612±32	0.096

[a] Equal variance test failed – *p* calculated using 1 way ANOVA on Ranks

3- Histomorphometry (Table 4)

Statistical analysis of the histomorphometrics results are presented in table 4 and graphically illustrated in figures 20, 21, 22, 23, and 24. Histological analysis demonstrated that HBO treated Non-Grafted defects had significantly more new bone ($p<.001$) and marrow ($p<.05$) and less fibrous tissue ($p<.05$) than Non-Grafted defects exposed to normobaric air. Defects grafted with autogenous bone showed no statistical differences in any of the parameters measured. Lesser amount of residual graft was present in the HBO compared to HBO defects neared significance ($p=0.085$) (Figure 23).

As expected in the normobaric defects, there was significantly more new bone and marrow and less fibrous tissue in the grafted defects ($p<.05$). However comparing the Non-Grafted and autogenous bone grafted defects in the HBO treated animals there was no significant difference in the amount of new bone ($p=0.196$), although there was less marrow and more fibrous tissue in the Non-Grafted defects ($p<.05$).

Table 4: Histomorphometric Analysis is demonstrated among the study groups and statistically analyzed using 1-Way ANOVA

| Type of Tissue (%) | NBO | | HBO | | 1-Way ANOVA |
	Non-Grafted	ABG	Non-Grafted	ABG	p value between groups
New Bone	19.7±2.6	36.6±8.6	46.7±5.3	41.4±6.9	<0.001
Marrow	6.3±3.6	37.8±9.1	26.7±9.0	38.7±5.7	0.004[a]
B+M	26.0±2.7	74.4±8.1	73.5±12.5	80.1±5.5	0.008[b]
Fibrous	74.0±2.7	6.4±1.8	26.5±12.5	8.8±6.1	<0.001[b]
Graft	N/A	19.1±7.7	N/A	11.2±4.7	0.085[c]

[a] Data not normal, p value generated by 1-way ANOVA on Ranks

[b] Data not equal variance, *p* value generated by 1-way ANOVA on Ranks

[c] *p* value for residual graft was determined by T-test.
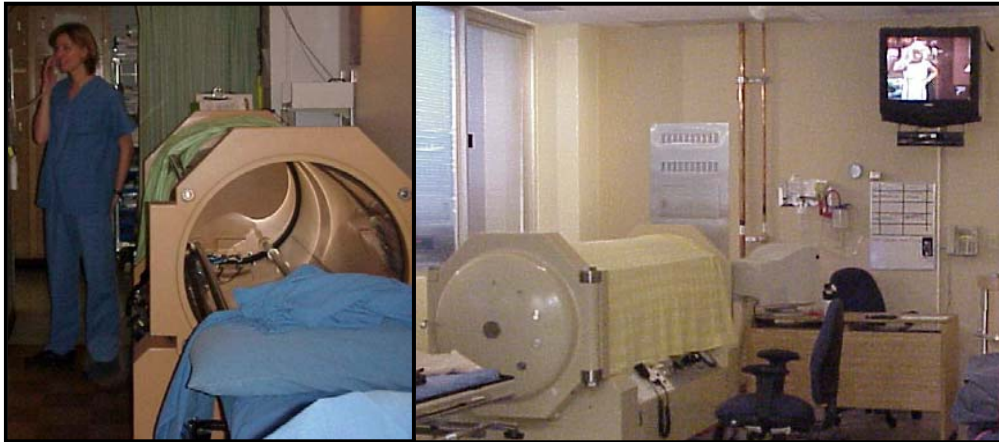
Figure 1: Monoplace chamber can only be utilized to treat one patient at a time. It contains compressed oxygen and is designed to treat individual patients one at a time
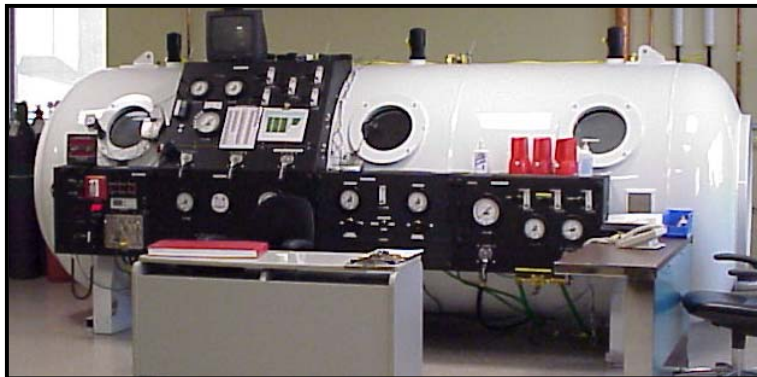

Figure 2: Multi-place chamber contains compressed room air. Multiple patients can be treated simultaneously while a trained attendant is monitoring the patients in the chamber. Patients breath 100% compressed oxygen through hoods or masks while sitting in the chamber.
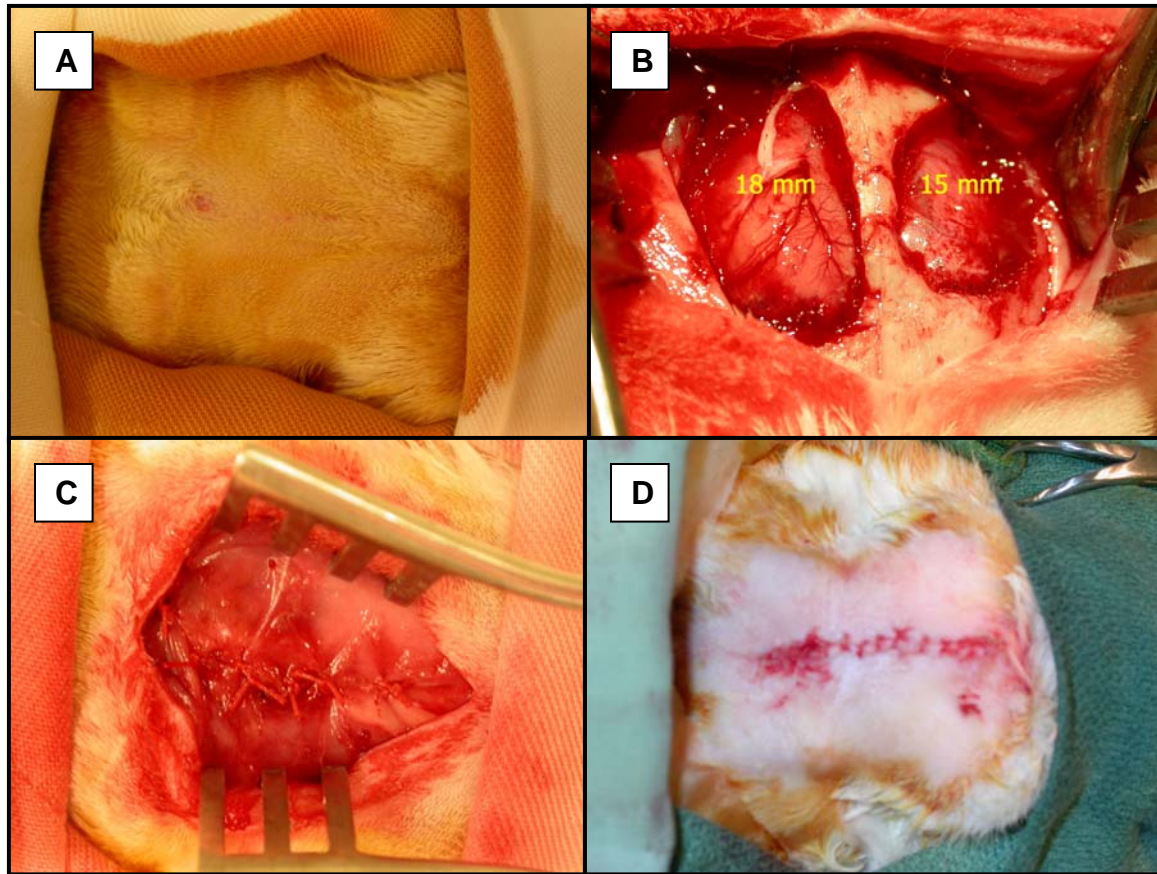
Figure 3: Phase I surgical protocol. A; Animal is in the prone position, prepped and draped. B; Full thickness osseous defect measures 15 mm (critical-sized) on one side and 18 mm (supracritical-sized) on the contralateral side. C; Pericranium is closed with 4-0 vicryl. D; Water tight closure for the skin.

Figure 4: Hyperbaric oxygen chamber specially designed for animal research. Rear end glass window permits animal monitoring using the mirror behind the chamber.
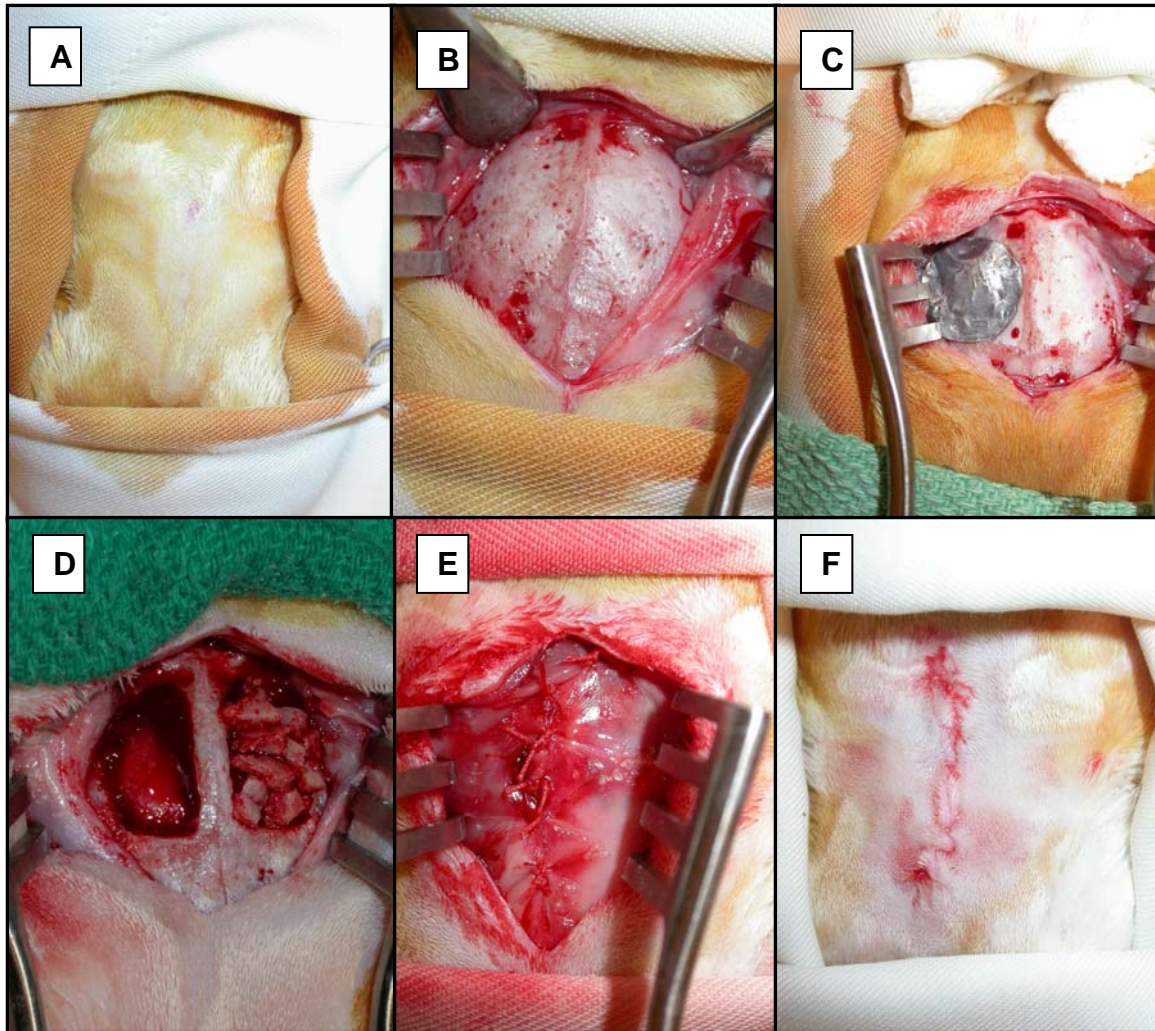
Figure 5: The surgical protocol for phase II. A; Animal is in the prone position, prepped and draped. B; Full thickness flap elevated and retracted by self retaining retractor. C; The surgical template measured 15x15mm to guide the osteotomy. D; Full thickness osseous defects created. One side filled with particulate autogenous bone graft. E; pericranium closed. F; Water tight closure for the skin.
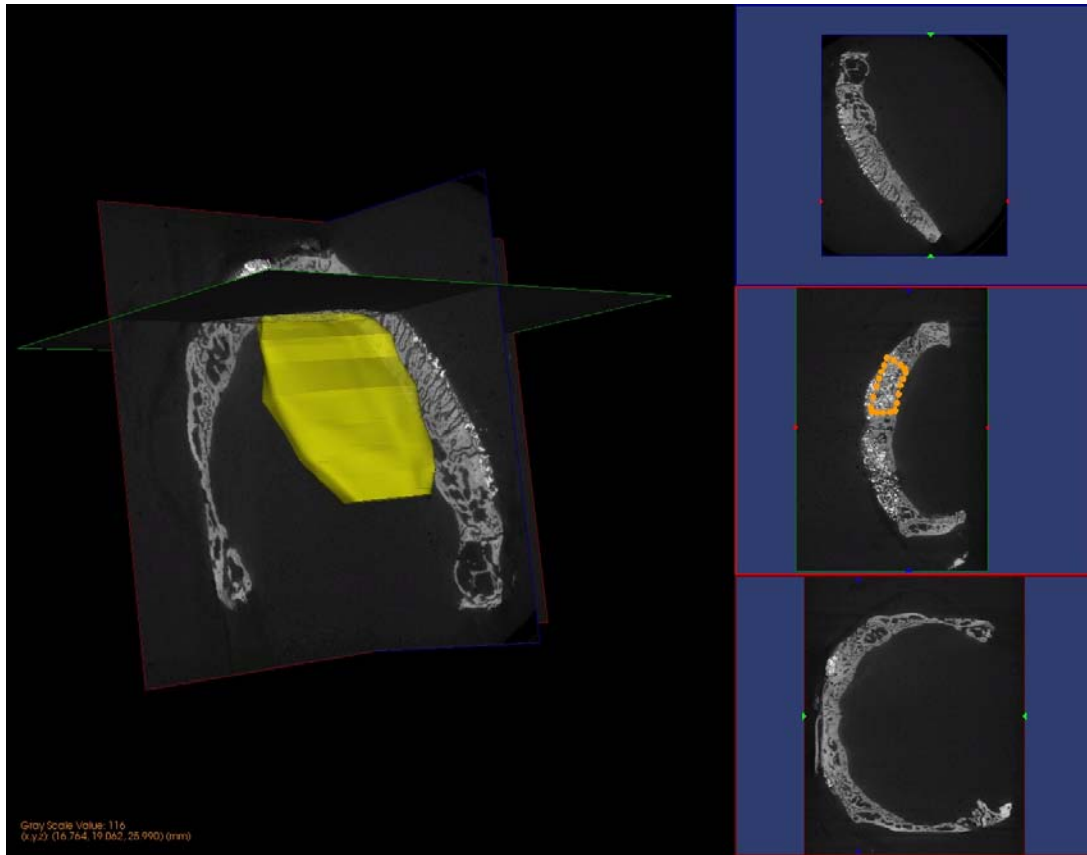
Figure 6: Micro Computed Tomography Coronal sections represent a defect traced in multiple sections. Tracings were interpolated generating a region of interest (ROI) which is shaded in yellow. The ROI was analyzed for total volume, bone volume, bone mineral content, and tissue mineral content.
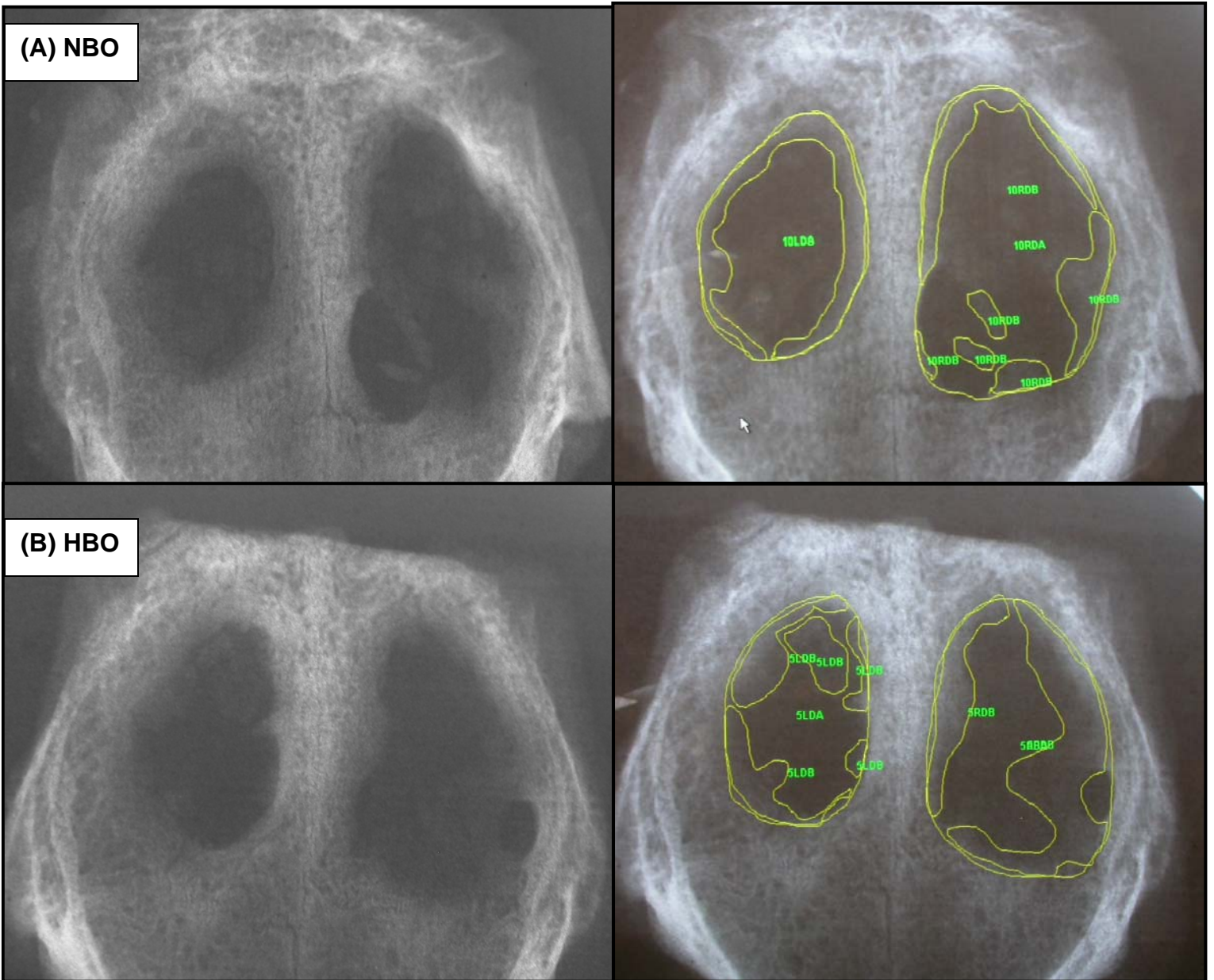
Figure 7: Postsacrifice radiographs of the parietal bones of A, Normobaric (NBO) group animal and B, HBO treated group animal. Tracing of apparent radiopacities indicates bone formation within defects.
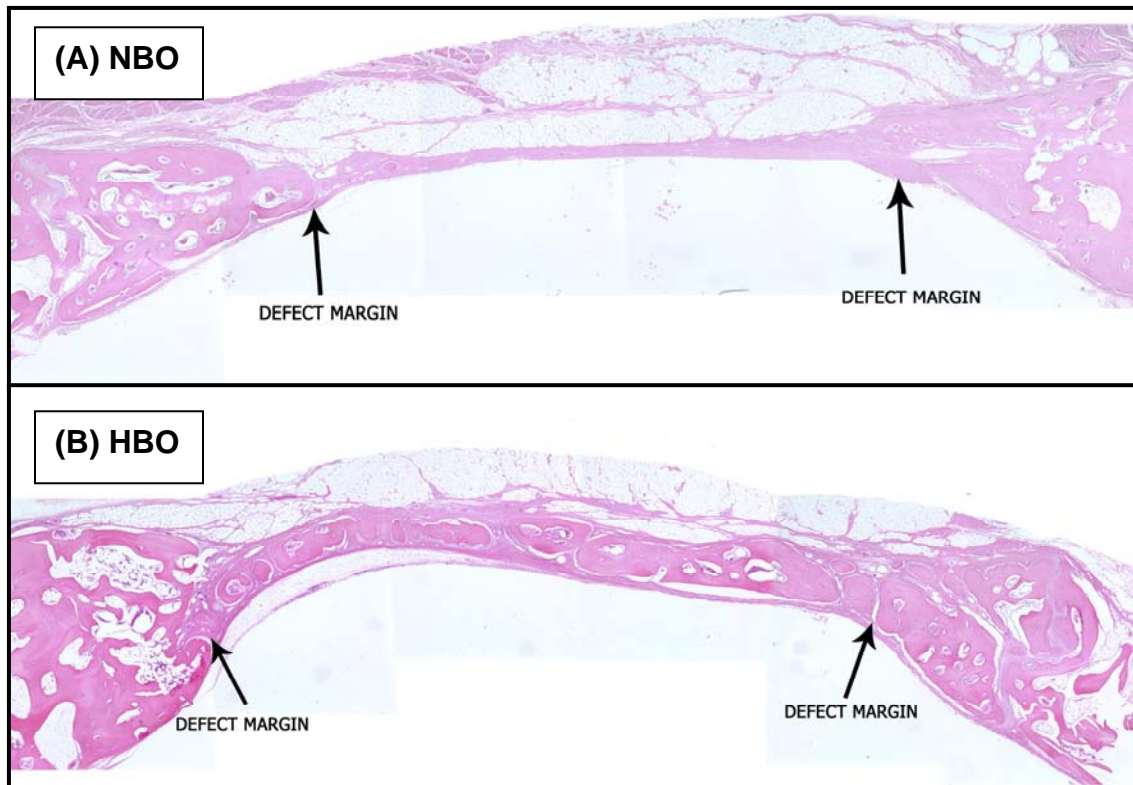
Figure 8: Histological Sections of HBO and NBO defects. 4X magnification hematoxylin and eosin stained sections. A, A normobaric (NBO) control group specimen healed primarily with fibrous band of tissue. B, An HBO treated animal sample showing bony healing of the defect.

(HBO = hyperbaric oxygen, NBO = normobaric room air oxygen).
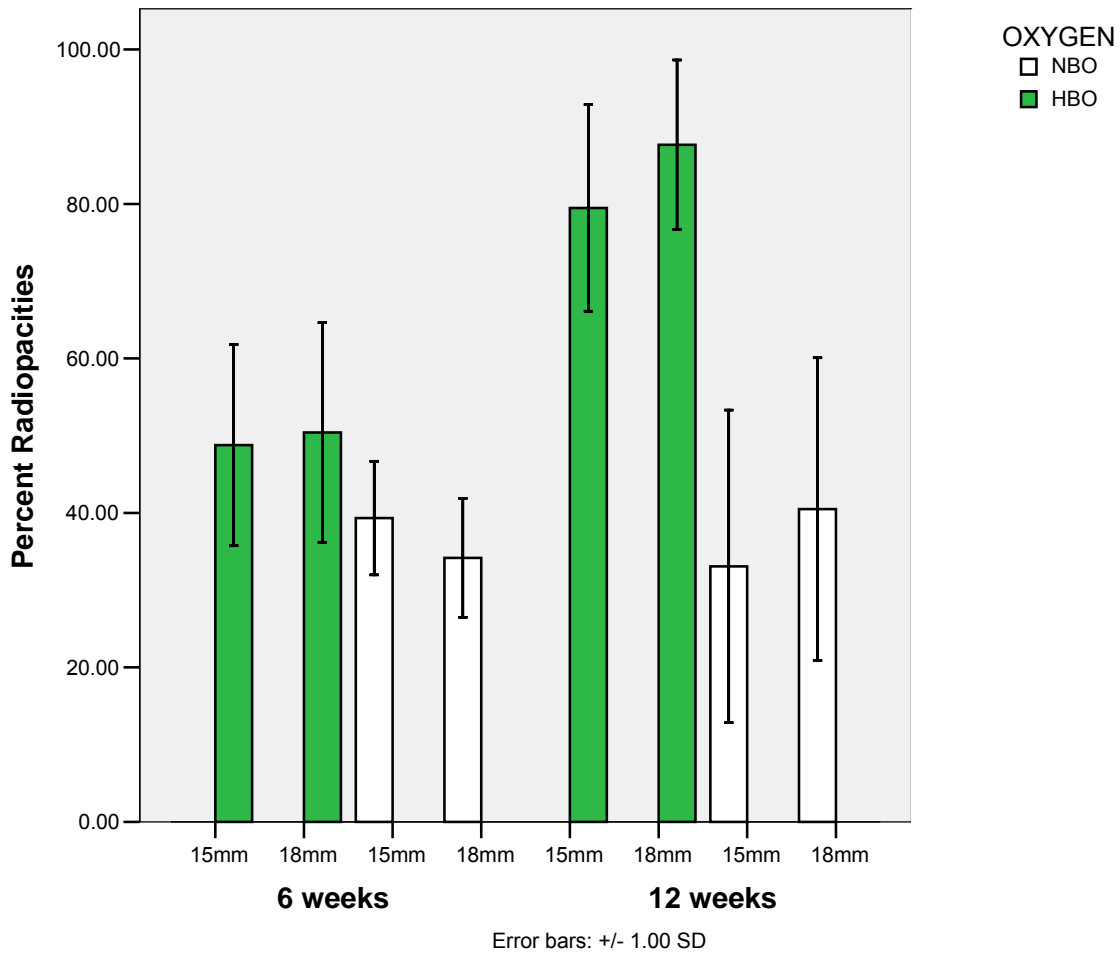
Figure 9: Bar chart, Radiomorphometrics. More mean percent radiopacities within the 15 mm and 18mm defects in the HBO group of phase I study (p<.001). More radiopacities were evident at the 12 weeks samples in the HBO group (p=.019).

(HBO = hyperbaric oxygen, NBO = normobaric room air oxygen)

Data is plotted as mean±SD.
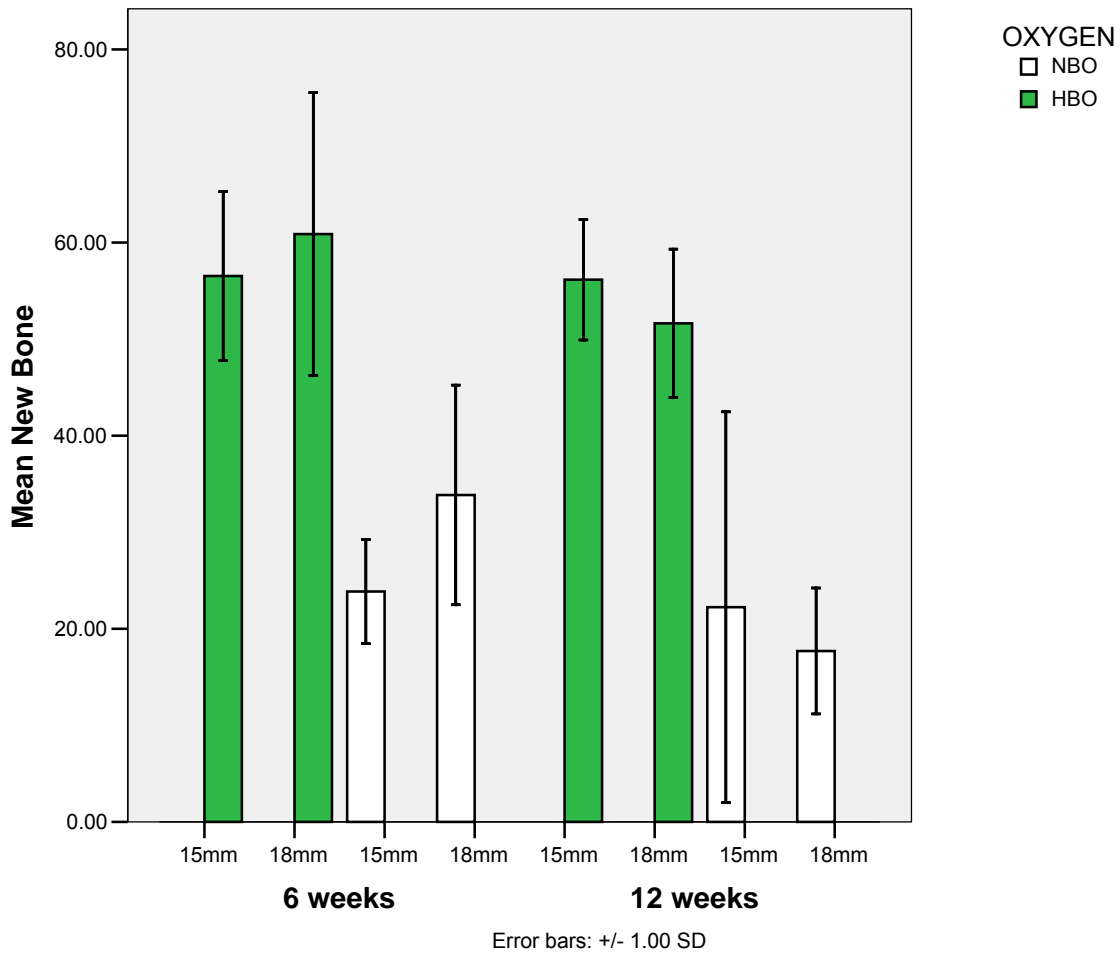
Figure10: Bar chart, Histomorphometrics New bone formation. Differences in the means of new bone formation based on histomorphometric measurements in the study groups. More new bone was evident in the HBO treated defects ($p<.001$).

(HBO = hyperbaric oxygen, NBO = normobaric room air oxygen).

Data is plotted as mean±SD.
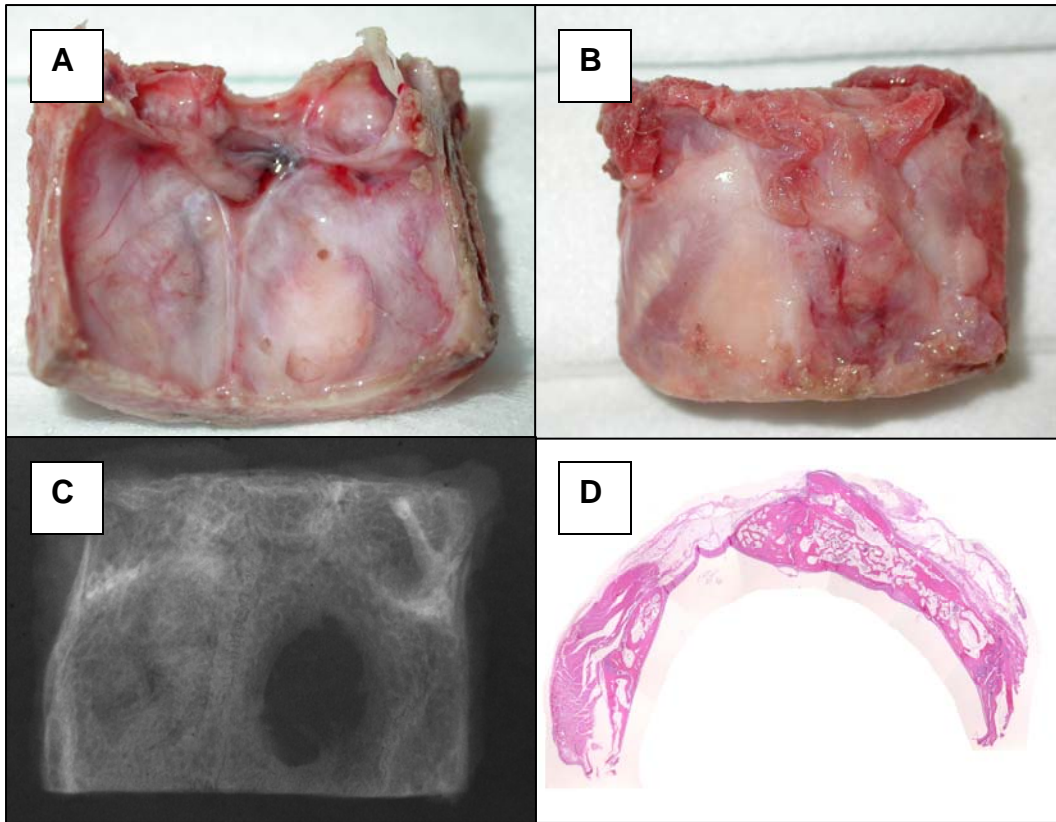
Figure 11: Normobaric Room Air Oxygen Defects. A; Gross specimen showing the inner or cranial surface. B; The outer surface of the specimen. C; Plain radiograph of the specimen is showing both defects. D; 7µm section is showing the fibrous union of the unfilled defect and bony union of the grafted defect.

(HBO = hyperbaric oxygen, NBO = normobaric room air oxygen).
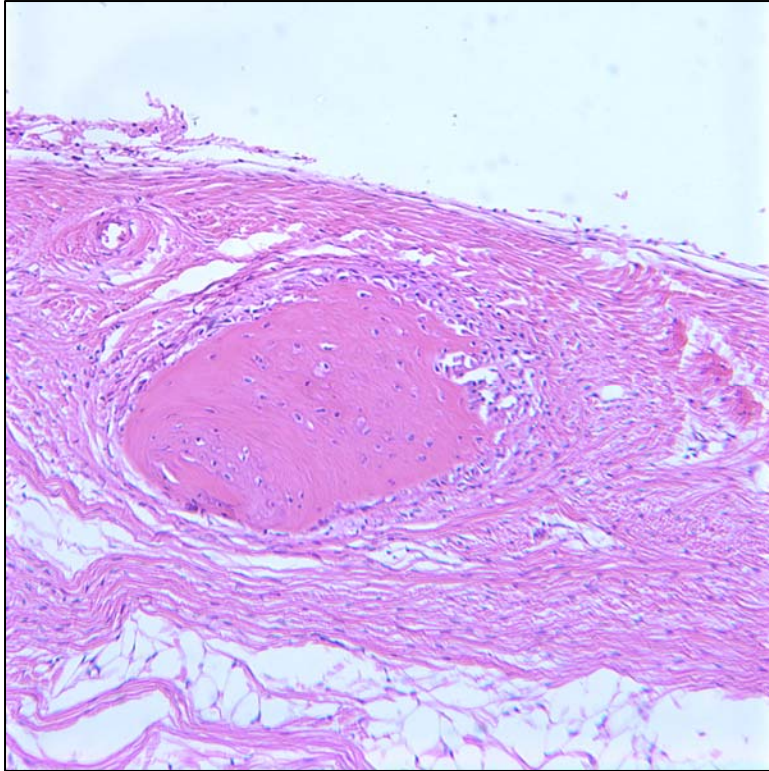
Figure 12: Histological section X20 of Non-Grafted rabbit calvarial defect from the normobaric group. These defects were mostly filled with fibrous tissue, with the occasional areas of bone formation and very little marrow.
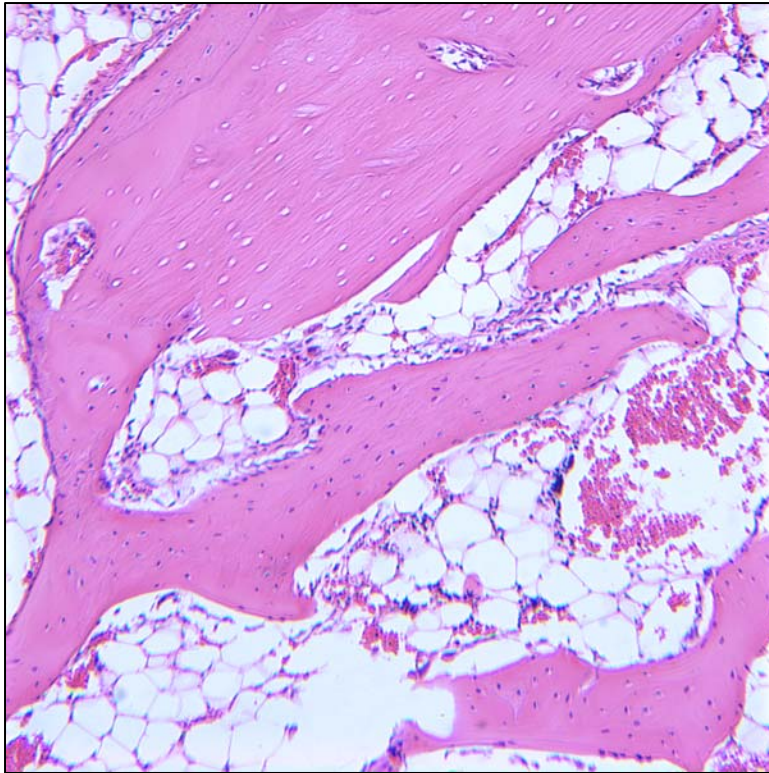
Figure 13: Histological section X20 of Grafted rabbit calvarial defect from normobaric group. Trabeculae of new bone formed around and sometimes incorporated the residual autogenous bone graft (ABG). The ABG could be clearly distinguished from the new bone due to the empty osteocyte lacunae. Extensive marrow is present throughout the defect.
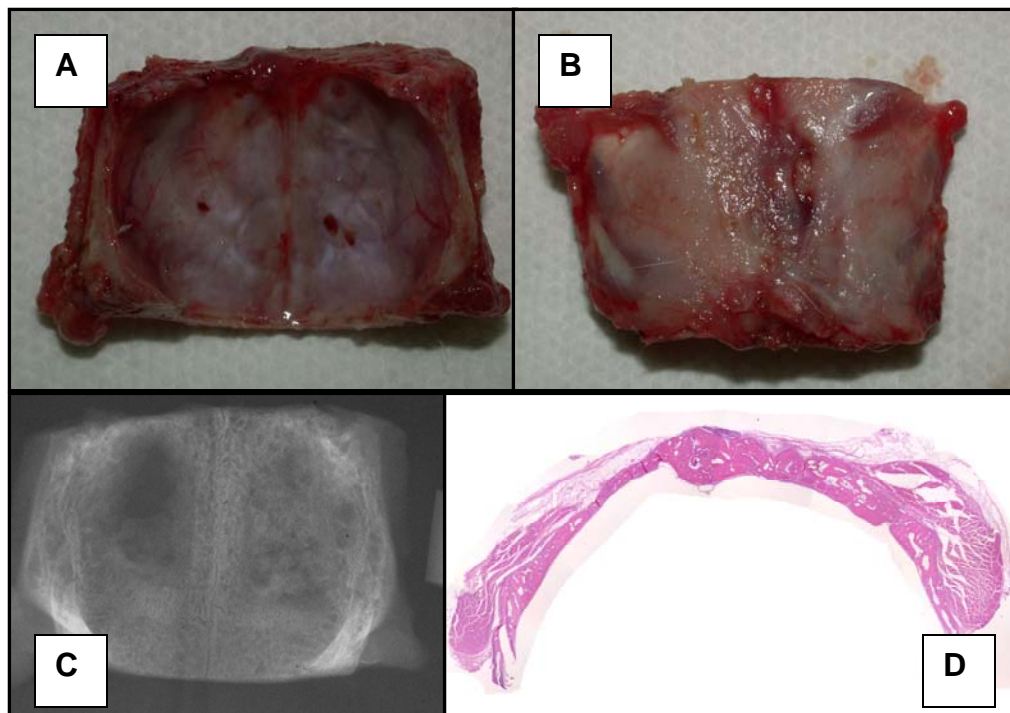
Figure 14: Hyperbaric oxygen treated defects. A; Gross specimen is showing cranial surface. B; The outer surface of the specimen. C; Plain radiograph of the specimen is showing both defects. More density in the Non-Grafted defect can be observed. D; 7µm section showing the bony union of both the Non-Grafted defect and the grafted defect. The Non-Grafted defect has however a thinner bony bridge.

Figure 15: Histological section X20 of Non-grafted defects exposed to hyperbaric oxygen conditions. Thick blocks of new bone are surrounded by dense fibrous tissue. Only small amounts of marrow are seen within the new bone.
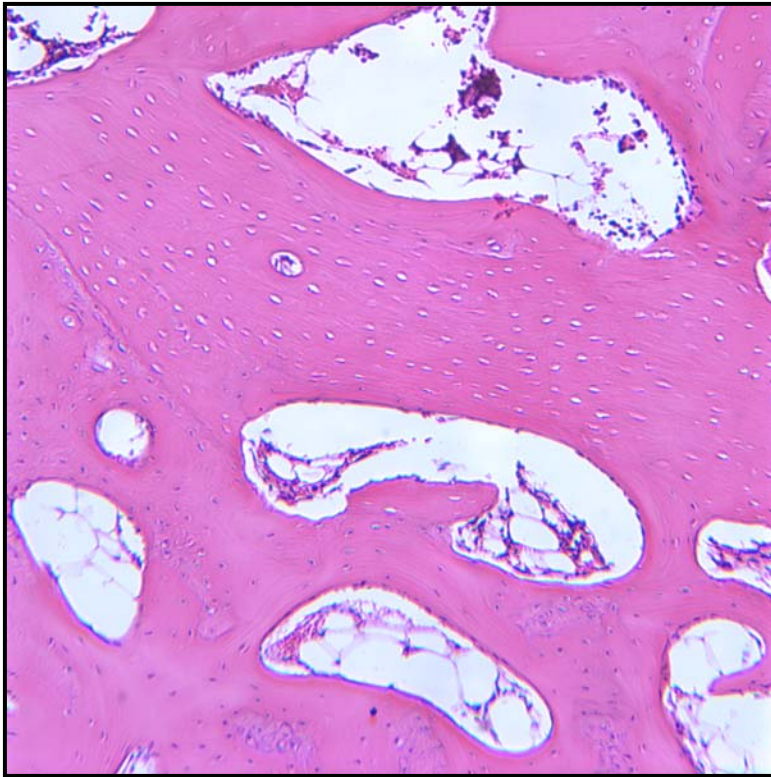
Figure 16: Histological section X20 of Grafted defects exposed to hyperbaric oxygen conditions. New bone forms along with and merges into the residual graft matrix. The remaining space is filled with marrow. No fibrous tissue is visible.
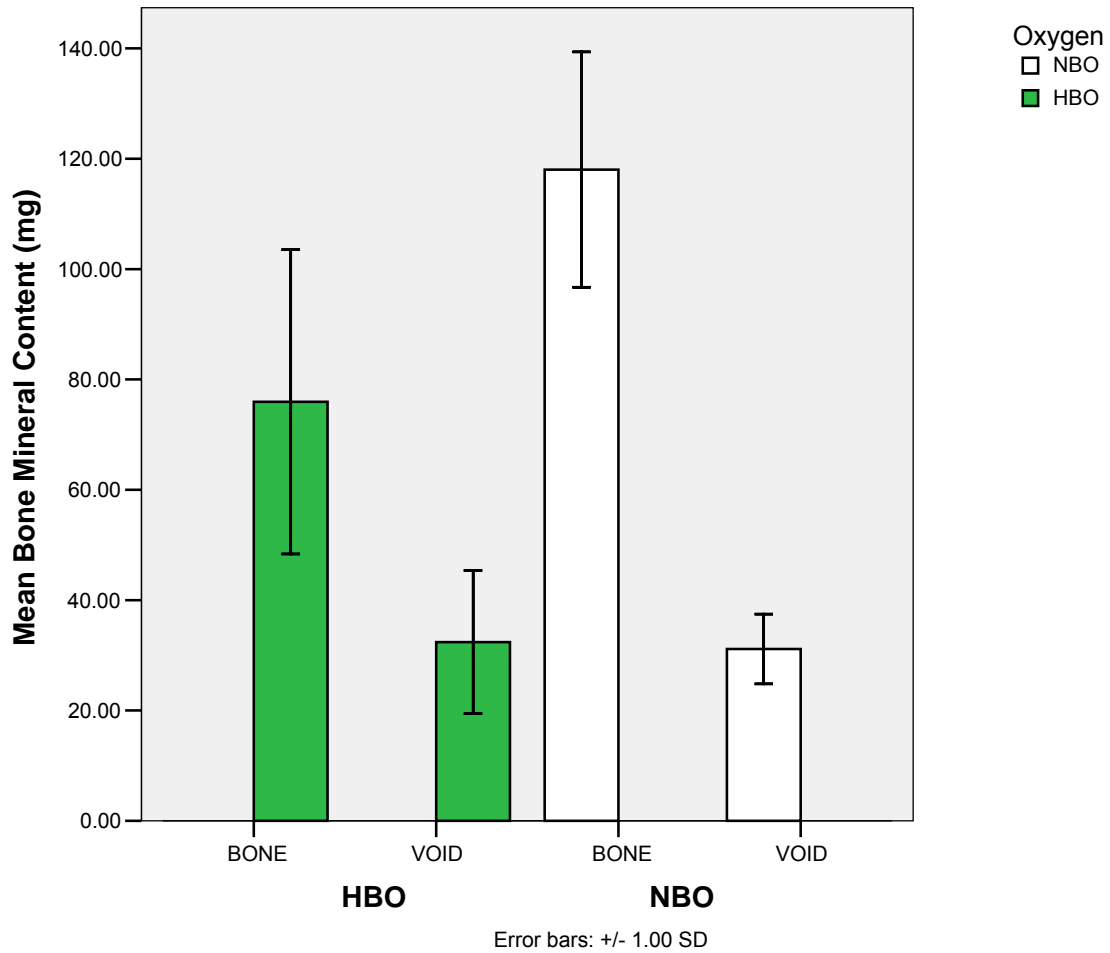
Figure 17: Bar Chart, Micro CT Results. Bone Mineral Content (BMC). The defects containing autogenous bone grafts have significantly higher BMC than the non-grafted defects (p<.05). Comparisons between the HBO and NBO autogenous bone grafted defects revealed that the HBO grafted defects had significantly lower BMC (p<.05). Data is plotted as mean±SD.
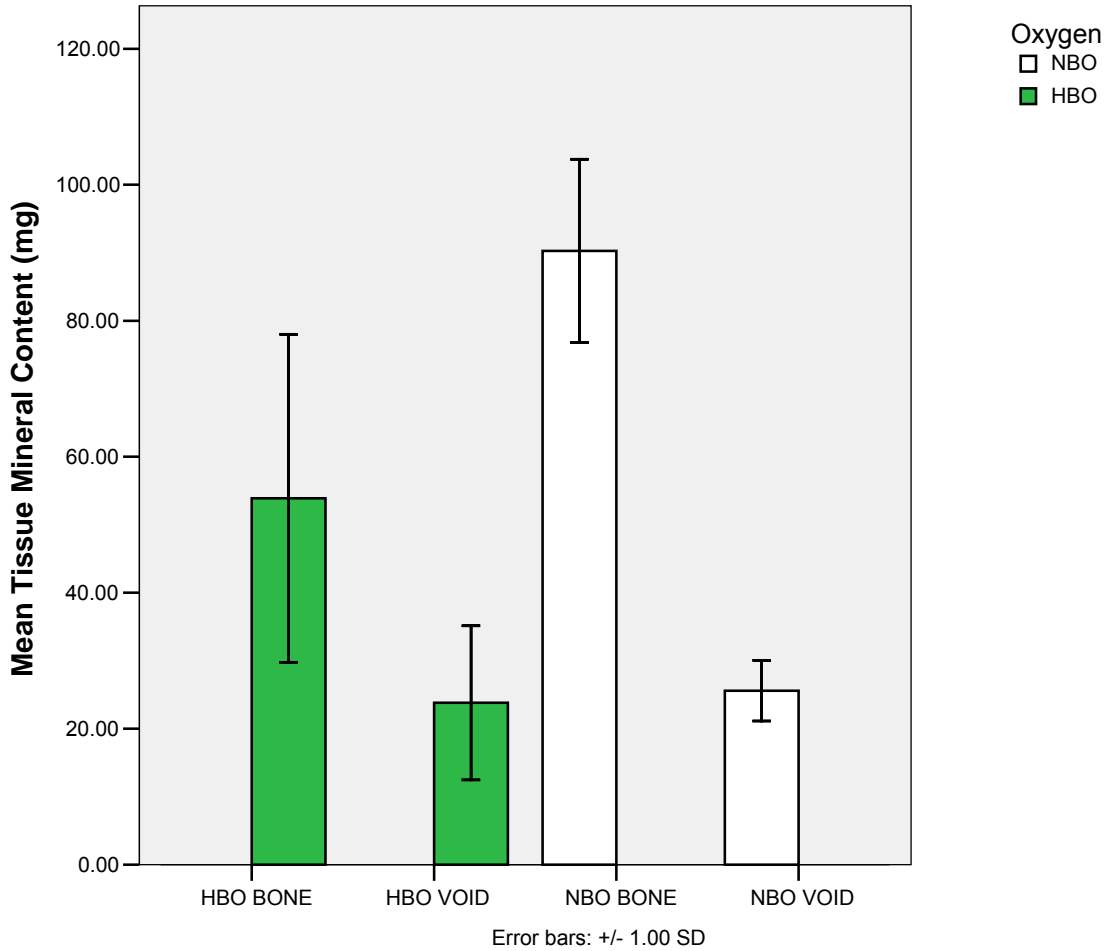
Figure 18: Bar Chart, Micro CT Results. Tissue Mineral Content (TMC). The defects containing autogenous bone grafts have significantly higher TMC than the non-grafted defects ($p<.05$). Comparisons between the HBO and NBO autogenous bone grafted defects revealed that the HBO grafted defects had significantly lower TMC ($p=.002$) Data is plotted as mean±SD.
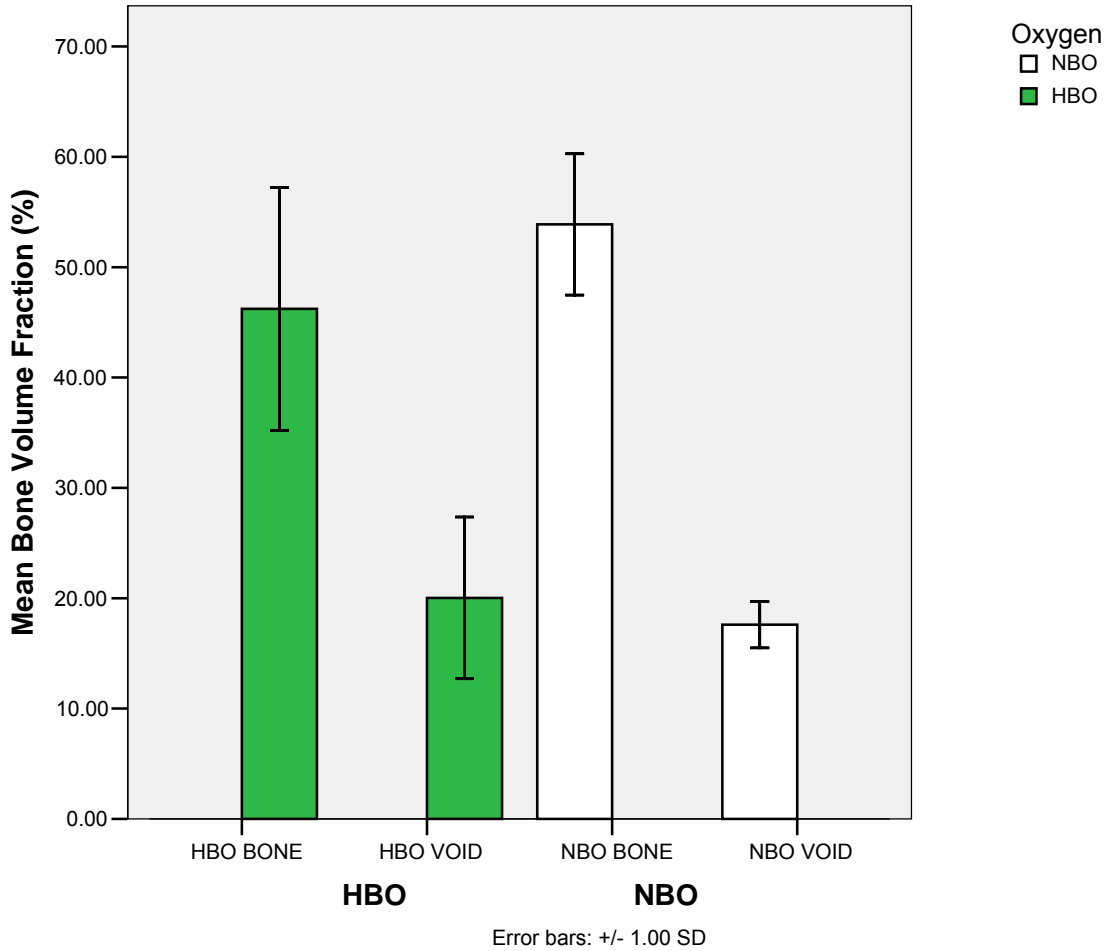
Figure 19: Bar Chart, Micro CT Results. Bone Volume Fraction (BVF). The defects containing autogenous bone grafts have significantly higher BVF than the non-grafted defects ($p<.05$). Comparisons between the HBO and NBO autogenous bone grafted defects revealed reductions in BVF in HBO grafted defects, however, this did not reach statistical significance ($p=0.123$). No significant differences between the HBO and NBO Non-Grafted defects were seen in this parameter.

Data is plotted as mean±SD.
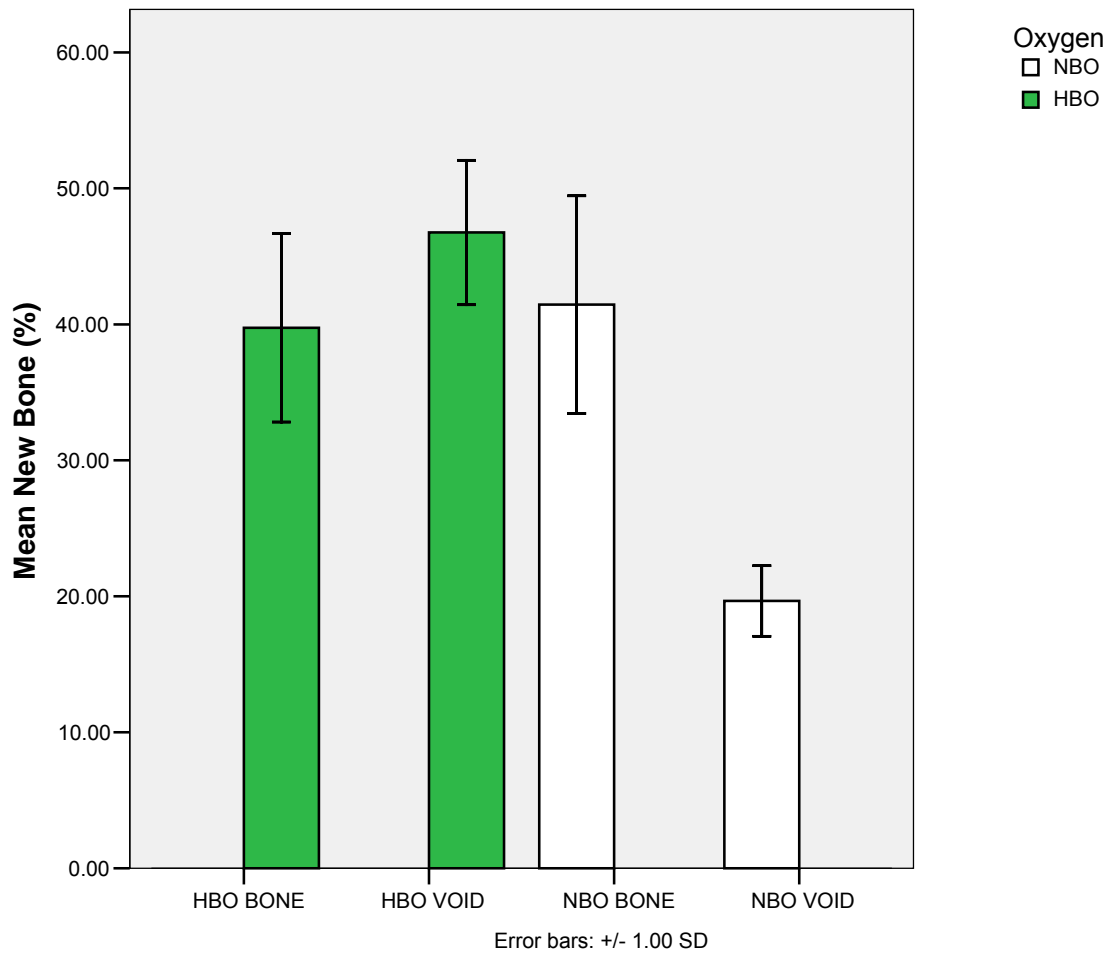
Figure 20: Bar Chart, Histomorphometry, New Bone Formation. HBO treated Non-Grafted defects had significantly more new bone (*p*<.001) than Non-Grafted defects exposed to normobaric air. Comparing the Non-Grafted and Autogenous Bone Grafted defects in the HBO treated animals there was no significant difference in the amount of new bone (*p*=0.196).

Data is plotted as mean±SD.
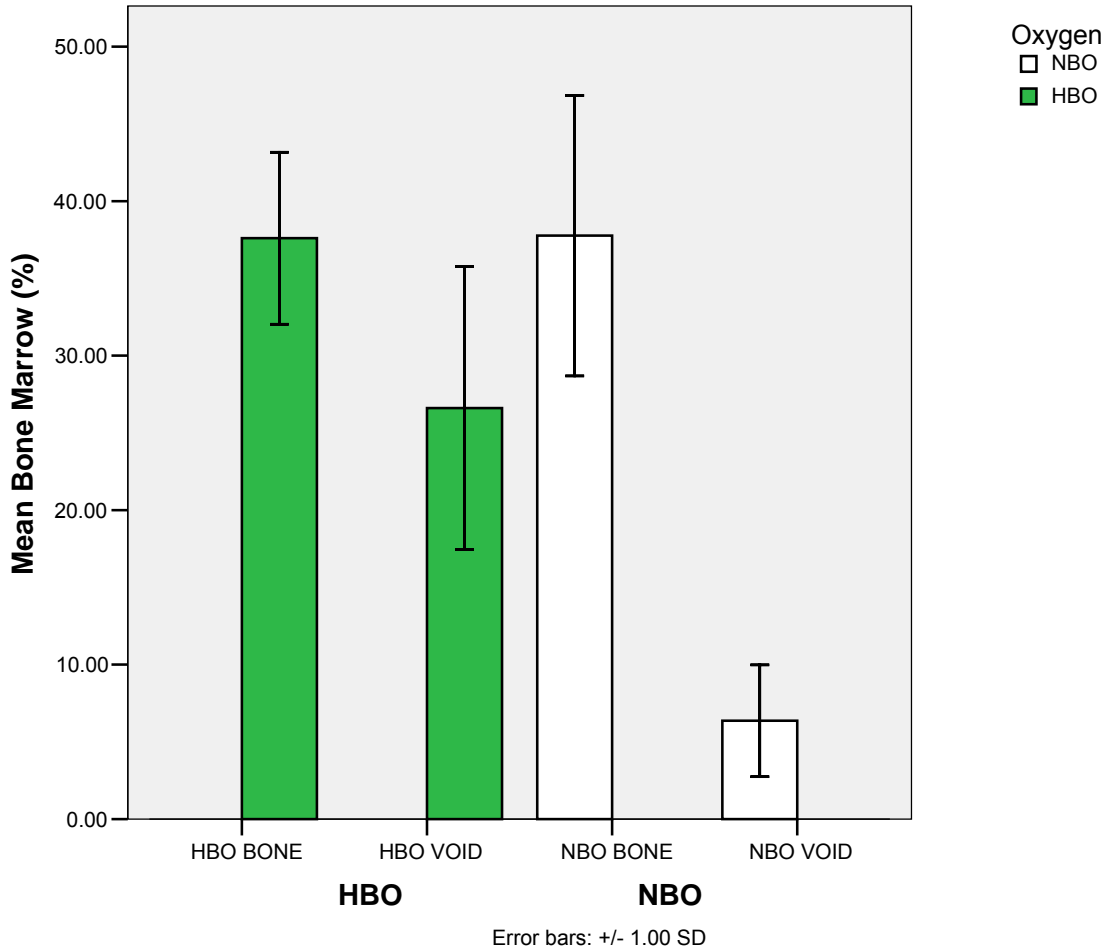
Figure 21: Bar Chart, Histomorphometry, Bone Marrow Formation. HBO treated Non-Grafted defects had significantly more bone marrow (*p*<.05) than Non-Grafted defects exposed to normobaric air. When comparing the Non-Grafted and autogenous bone grafted defects in the HBO treated animals, there was less marrow in the Non-Grafted defects (*p*<.05).

Data is plotted as mean±SD.
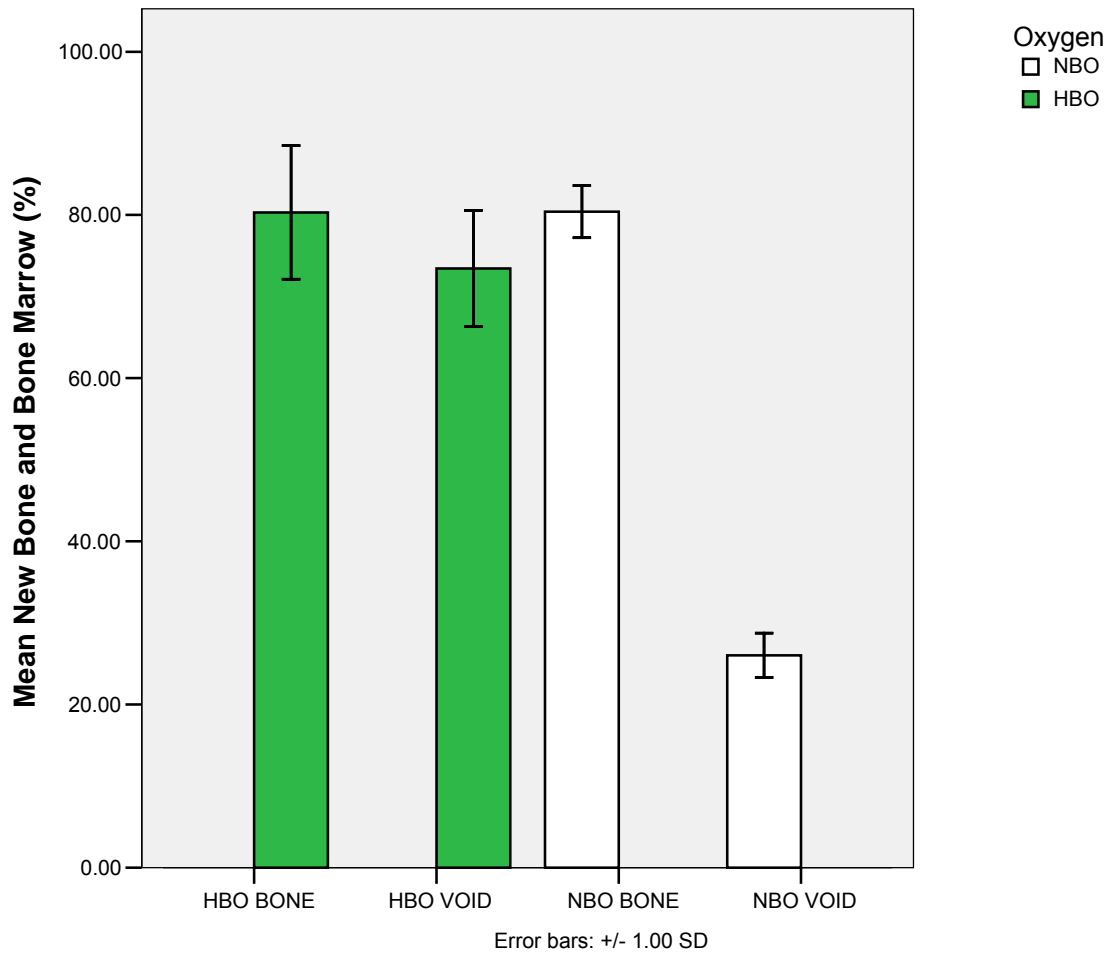
Figure 22: Bar Chart, Histomorphometry, New Bone Formation and New Bone Marrow Formation Combined. Significantly less new bone and marrow were observed in the void defects exposed to normobaric air when compared to the other 3 types of defects (p=0.008). HBO void defects and grafted defects formed comparable amounts of new bone and new marrow.

Data is plotted as mean±SD.
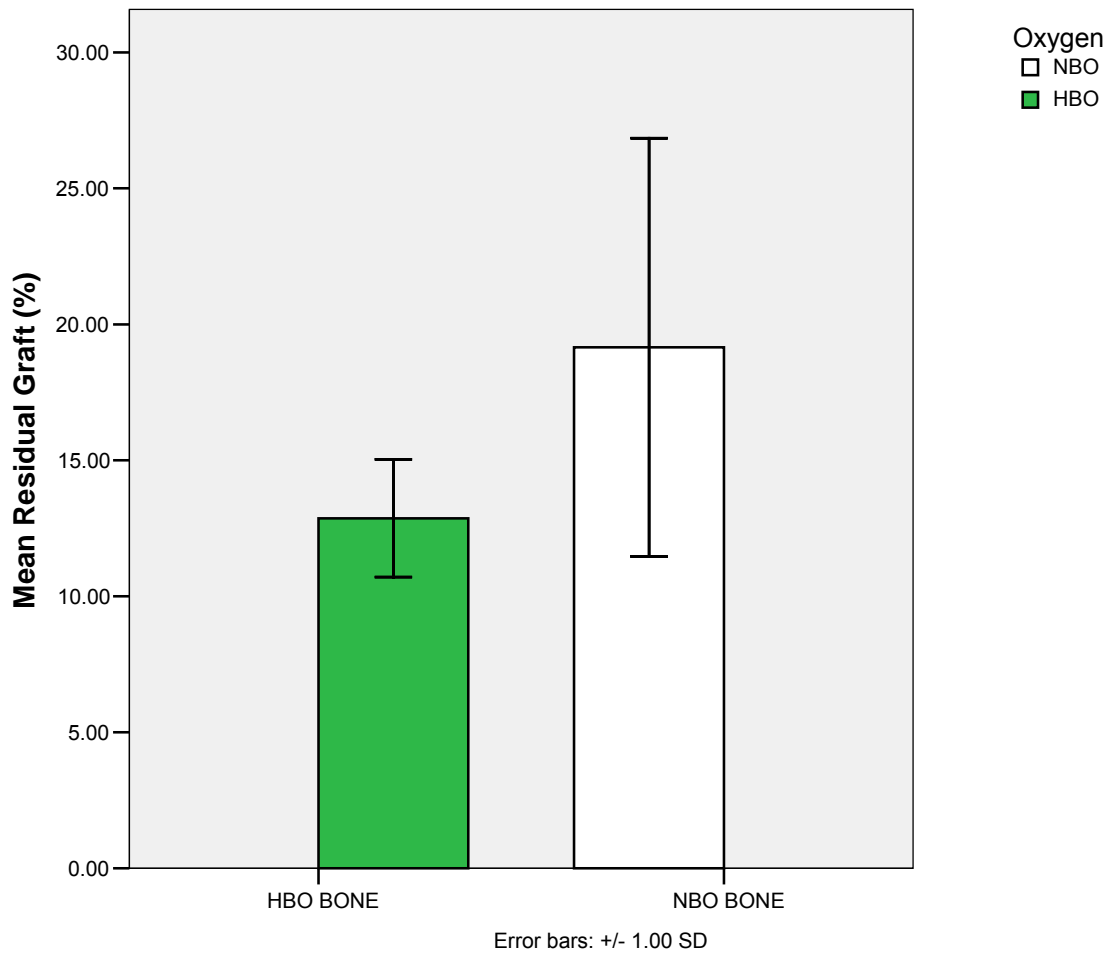
Figure 23: Bar Chart, Histomorphometry, Residual Graft. The lesser amount of residual graft present in the HBO compared to NBO defects neared significance (p=0.085).

Data is plotted as mean±SD.
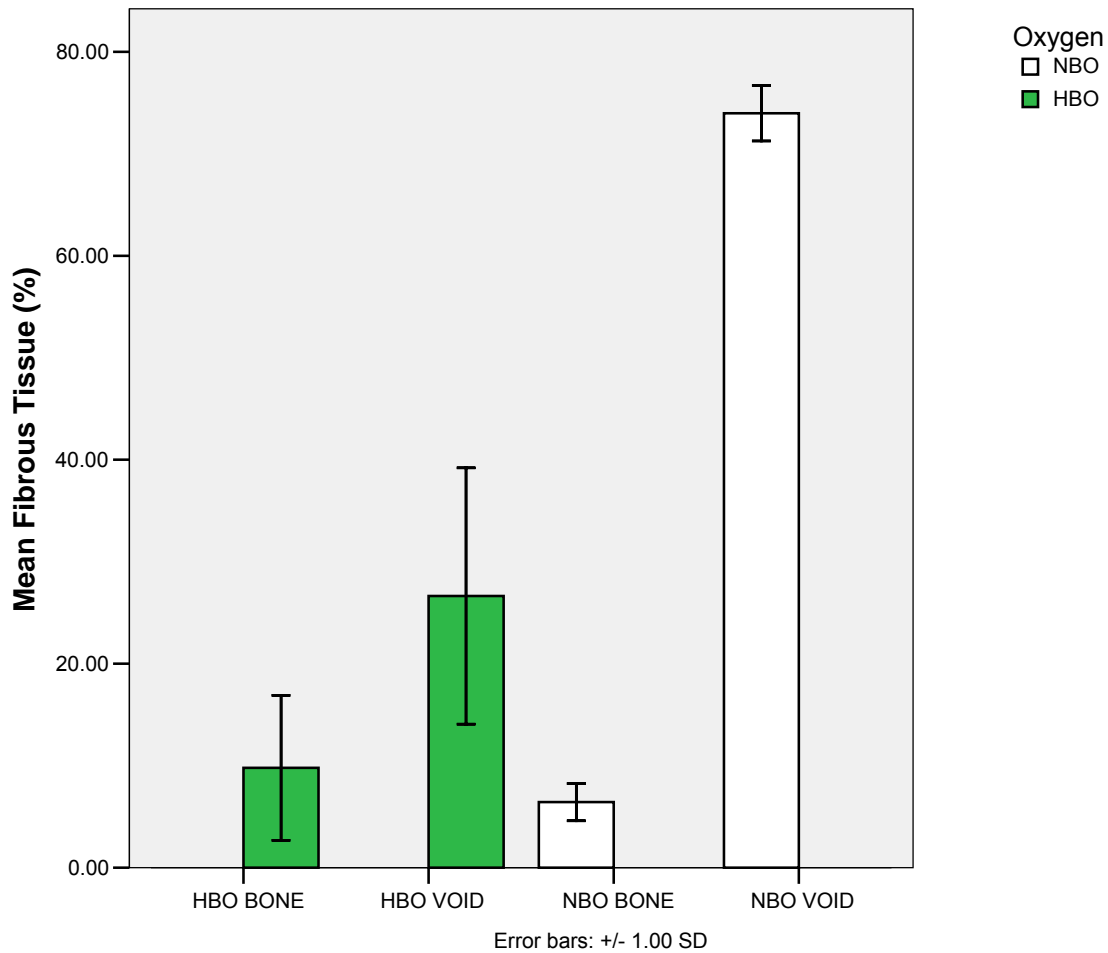
Figure 24: Bar Chart, Histomorphometry, Fibrous Tissue Formation. Significantly less fibrous tissue (*p*<.05) was detected in the HBO treated defects. Void defects exposed to normobaric air healed mostly with fibrous tissue.

Data is plotted as mean±SD.

Chapter V: Discussion

Our main interest for conducting this investigation was to study the influence of Hyperbaric Oxygen (HBO) on the healing of critical sized defects. The goal of this investigation was to inquire if HBO can change the accepted critical size of full thickness calvarial wound model. A second goal was to question bone regeneration in the absence of bone grafting and whether this was comparable to the gold standard, which is autogenous bone grafting. Results of this two phase investigation were interesting in that we were able to demonstrate bony union in critical sized defects treated with HBO in the absence of bone grafting. HBO increases the critical size of the calvarial defect model in rabbits to more than 20%. Moreover, the regenerate has new bone quantity that is equivalent to autogenous bone grafting.

Reconstruction of large defects in the maxillofacial skeleton has been always a challenging problem facing oral and maxillofacial surgeons. The current "gold standard" for the treatment of bony defects which are unable to heal spontaneously (critical-sized defects) is the use of autogenous bone grafts. However the volume of bone available for grafting is limited and the use of large grafts results in significant complications including donor site morbidity and extended time in surgery.

Microvascular osseous flaps provide an attractive option. They have the advantage of providing the graft with its own blood supply (Ang et al., 2003). Harvesting microvascular osseous flaps can result in significant morbidity of the donor site. Free autogenous bone grafting techniques are readily available options for oral and maxillofacial surgeons and are associated with fewer donor-site complications. A crucial requirement is the availability of adequately vascularized soft tissue bed to promote

neoangiogenesis, to maintain graft viability and phase I bone graft healing. This lack of neoangiogenesis can be a limiting factor in patients who have received radiotherapy as part of a malignant disease management regimen. An aggressive infectious condition may also jeopardize the soft tissue bed and compromise the healing of an autogenous non vascularized bone graft (Jisander, Grenthe & Salemark, 1999).

Although complications from a posterior ilium bone graft harvest are uncommon and seldom can cause permanent disability, donor site morbidity can occasionally be disabling and discouraging for patients going through reconstructive surgical procedures. A review of 839 posterior iliac crest bone graft harvests revealed that the incidence of fractures was very low (0.2%). Seroma was a common complication (3.6%) in which only 0.7% of cases required surgical intervention. Permanent gait disturbance rate was low (0.5%). None of the patients had disturbing dysesthesia (Marx, 2005). Yet, not all patients are suitable to go through this surgical procedure. We were able to demonstrate that HBO promote bone regeneration in defects 20% larger than the critical sized defect in the absence of autogenous bone grafting. Hence HBO may reduce the required amount of bone to reconstruct those defects. This may introduce a key element in maxillofacial reconstructive techniques.

Hyperbaric oxygen therapy (HBO) has been used with success in the treatment of hypoxic wounds and in anoxic conditions. Moreover, HBO has been observed to significantly increase bone formation in the rabbit bone harvest chamber (Nilsson et al., 1988). Our findings agrees with those of Nilsson et al. 60% bone formation was detected in HBO non-grafted defects which is significantly higher than the normobaric room air controls ($p<.001$).

The undersea and hyperbaric medicine society (UHMS) has approved several medical indications for HBO therapy that relate to Oral and Maxillofacial surgery (Broussard, 2004) including enhancement of healing in problem wounds, necrotizing soft tissue infections, refractory osteomyelitis, radiation induced necrosis, and compromised skin grafts and flaps. Although Hyperbaric oxygen therapy is costly, the potential cost must be weighed against savings that may be realized from improved tissue healing and reduction of complicated outcomes such as flap or graft failure (Attinger et al., 2008).

The rabbit calvarial critical-sized defect model is similar to clinical maxillofacial reconstruction in many respects. Calvarial defects are full thickness osseous defects with a periosteal blood supply. The membranous origin of the bone and the pattern of bone healing are other similarities. One difference, however, is the presence of a pulsatile dural layer in the base of the rabbit calvarial model, which is not present in extracranial maxillofacial wounds. Nevertheless, none of the specimens showed any clinically significant bowing or cranialization of the defects. That is most likely due the preservation of the dural layer.

The minimum size of the defects used in this study was 15-mm in diameter. This was defined as a critical-sized defect by Schmitz and Hollinger in 1986 (Schmitz & Hollinger, 1986). Their definition described these defects as full thickness defects that would not heal spontaneously during the lifetime of an animal. This was revised by Hollinger and Kleinschmidt in 1990 to be a defect having at most 10% of bony healing 10 years postoperatively (Hollinger & Kleinschmidt, 1990). Supracritical-sized defects of 18 mm were also studied in phase I and demonstrated bony healing after 6 weeks and

12 weeks time periods. The mean bone formation was 60.88±14.65 and 51.64±7.67

respectively. Further increases in the size of the defect beyond 18-mm would have

required crossing the midline of the cranial vault, which posed a significant risk of lethal

hemorrhage by potentially violating the sagittal sinus. Extending the defect to involve

the temporal and the frontal bones might have altered the healing due to the

involvement of the sutures. However, since the subjects were all skeletally mature, the

sutures were expected to be fused. Hence, the calvarium can be considered as a single

unit. Extending the defect laterally may endanger the sphenoparietal venous sinus.

Removing larger amounts of bone than required to produce an 18 mm supracritical-

sized defect may render the calvarium structurally unsound and incompatible with life

for the animal

One of the aims of these two studies was to evaluate the effects of HBO on

osseous wound healing and to determine if HBO can facilitate bony repair of critical

sized defects. Hyperbaric oxygen therapy (HBO) has been shown to promote the

healing of Non-Grafted critical-sized defects in rabbits. Histomorphometric analysis

revealed significantly more bony healing in HBO treated defects ($p<.001$). Both critical-

sized 15 mm and supracritical-sized 18 mm defects healed with significantly more bone

in the HBO group when compared with the control normobaric group. This change in the

potential healing of critical sized defects may introduce a modification to the definition

suggested by Hollinger as the smallest osseous wound that will not heal spontaneously

during the experimental period or the life of the animal (Hollinger et al., 1994). Host

systems induced healing via bony union with the aid of temporary intermittent hyperoxia

during the initial healing period. The previously accepted critical-size of calvarial defects may have increased from 15mm to more than 18mm.

Radiomorphometric analysis revealed significant differences in the percentage of radiopacities in the HBO group at 6 versus 12 weeks. However, this was not reflected in the histomorphometric measurements, where the amount of bone in the defects was unchanged between 6 and 12 weeks. This finding can be explained by the fact that actual bone that is demonstrated histologically will not necessarily be evident radiographically until it has matured and mineralized. Meanwhile, histological evaluation indicated a change in bone from woven to lamellar bone between 6 and 12 weeks, which would be expected to result in an increase in the radiodensity of the bone.

The 15mm defects exposed to normobaric room air exhibited excessive variance on radiomorphometric analysis. Mean radiopacities was 33.08±20.24. This high variance may be explained by collapse of the pericranium in some specimens preventing the formation of bone. One way that could have prevented this collapse is to apply a resorbable or non-resorbable membrane to guide for bone regeneration.

The process of acclimatizing the HBO group of rabbits to the chamber for one week prior to the surgical procedure reduced the discomfort of the rabbits to being confined in the chamber and thus minimized stress, which could have adversely affected healing. HBO therapy was applied intermittently to minimize the theoretical blockade of hypoxia and lactate induced collagen synthesis and neovascularization (Mainous, 1982), (Tuncay, Ho & Barber, 1994) as well as the differentiation of osteoprogenitor cells in the calvarial bone marrow and in the periosteal layer of the pericranium and the dura matter (Ozerdem et al., 2003). A total of 20 HBO sessions

were chosen because neovascularization was reported to reach a plateau by 20 sessions (Marx et al., 1985).

HBO seems to be an effective measure to enhance membranous bone healing in the rabbit calvarial critical sized defect model. The results reported here suggest that HBO treatment sessions as in the protocol described in this study significantly enhance bone formation within the critical-sized defect, even in the absence of an autograft or a bone substitute (Figures 8 and 10), possibly minimizing the amount or eliminating totally the bone graft required or bone substitute required permitting healing of bony calvarial critical-sized defects. HBO may be a useful replacement for autogenous grafts in certain instances such as patients with multiple comorbidities and with higher than average perioperative risks. As an adjunctive therapy to autogenous bone grafting, HBO may minimize the amount of graft required in other instances. In order to confirm the previous statement, the phase II study was designed to compare and contrast bone regenerated with the effect of hyperbaric oxygen alone versus the gold standard, which is particulate autogenous bone grafting. This conclusion from phase I initiated the aim of the second phase of this study; to evaluate the effect of HBO on the healing of critical-sized defects in the presence and absence of autogenous bone grafts in comparison to defect healing with grafts under normobaric conditions.

Phase II of this study demonstrated histologically that there was significantly more bone (p<.001) and marrow (p<.05) in the HBO treated Non-Grafted defect than the control Non-Grafted defects in untreated animals (Figures 20 and 21). These results are in agreement with the results of phase I of this study which investigated the effect of HBO on critical-sized defect healing. Interestingly we were unable to demonstrate this

68

difference in bone volume (BV) by micro CT bone analysis (Figure 19 and Table 3). The difference between micro CT bone volume analysis and histomorphometrics suggests that the newly formed bone at 6 weeks had not yet matured to become fully mineralized and detected by the software at the set threshold for intact bone. Thus, histomorphometrics remain the gold standard in assessing bone regeneration in critical-sized defects.

HBO therapy induced a reduction in Bone Volume (BV), Bone Mineral Content (BMC) and Tissue Mineral Content (TMC) in grafted defects. But the reduction in Bone Mineral Density (BMD) and Bone Volume Fraction (BVF) did not reach significance (p=0.123 and 0.078 respectively). The presence of the graft, expectedly, resulted in increased BV, BMC, BMD and BVF compared to Non-Grafted defects under both NBO and HBO (p<.05). It is difficult to explain the reduction in BMC in HBO Grafted defects especially considering the non-significant decrease in BMD and the significant increase in new bone histologically in HBO non-grafted defects. Increased osteoclastic activity and/or vascular ingrowth may account for the drop in BMC and TMC. In the setting of enhanced angiogenesis, more space may be occupied in the healing defect by blood vessels, contributing to an apparent fall in the relative amount of bone in the defect at this time point.

It was difficult to distinguish the defect margins in the Non-Grafted HBO treated defects. Defect margins were estimated through higher magnification and through observing abrupt change in the direction of lamellae. Radionuclide labeling could have been useful to label old bone at the time of surgery. Technetium 99 is a potential option but can be washed away during decalcification. Tetracycline is another potential option

but may not be desirable due to it permanent effects on new bone quality. Tritiated thymidine is the amino acid; thymidine linked to the radioisotope tritium; abbreviated 3HTdR. It is commonly used to label DNA synthesis. 3HTdR could be a useful radiolabeling method to differentiate old from new bone (Cei et al., 2006).

Histomorphometric comparison of the amounts of new bone excluding bone marrow in the HBO treated Non-Grafted defect and the Normobaric Autografted defects showed more bone in the HBO group that neared significance (46.7 ± 5.3 vs. 36.6 ± 8.6 p=0.054). Conversely there was significantly less marrow and more fibrous tissue in the HBO Non-Grafted defects than the NBO grafted defects (marrow: 26.7 ± 9.0 vs. 37.8 ± 9.1; p<.05; fibrous 26.5 ± 12.5 vs. 6.4 ± 1.8 p<.05). HBO was reported to increase fibroblast proliferation and expression of basic fibroblast growth factor (bFGF) (Kang et al., 2004). The increase in fibrous tissues was almost exclusive to the pericranial and dural sides of the HBO Non-Grafted defects. Observed in the NBO Non-Grafted defects, a fibrous tissue band was occupying the defect centrally with only occasional bony islands scattered around the lateral and medial edges of the defects. Since the sigma for rabbits on is only 6 weeks (Parfitt, 1976), no more bone was expected to form within the defects spontaneously after 6 weeks. However, an autogenous bone graft is expected to continue to mature and remodel to meet metabolic and functional demands of the calvarium. In other words, the higher percentage of bone marrow in NBO grafted defects compared to HBO Non-Grafted defects may normalize during phase II bone graft healing.

When the amount of bone and marrow are considered as a single measure of "reparative tissue" the amounts in the HBO Non-Grafted and NBO grafted defects were

almost identical (73.5±12.5 vs. 74.4±8.1) (Figure 22), with a volume equivalent to that occupied by residual graft in the NBO defects being occupied by fibrous tissue in the HBO treated defects. This suggests that HBO therapy alone enhances bone healing with a volume comparable to autogenous bone grafting. However, clinical and functional capabilities of bone regeneration in HBO treated non-grafted defects have yet to be examined, possibly through a loading implant model in critical-sized mandibular defects.

Differences between other sites must be kept in mind. The blood supply to a mandibular defect model might be quite different than the calvarial model. Vessels distribution and possible contribution of the inferior alveolar artery makes the mandibular model more vascular than the calvarial model. The facial artery as well as the lingual artery will also contribute to the difference in the blood supply. These differences must be kept in consideration when designing a loading model.

Histomorphometric comparison of the HBO and NBO defects that contained autogenous grafts revealed there were no significant differences, although the reduction in the amount of residual graft in the HBO group neared significance (11.2±4.7 vs. 19.1±7.7 p= 0.085). However, the micro CT bone analysis did show that there was a significant reduction in the bone mineral content of the defect (p<.05) and a near significant reduction in bone mineral density (p=0.078). The difference between the micro CT and histomorphometric results may indicate that there is increased resorption and/or demineralization of the residual graft, which would not be easily detected by histomorphometry. This reduction in bone mineral content might be attributed to increased osteoclastic activity and/or neoangiogenesis (Fok et al., 2008).

Fok et al demonstrated elevation of VEGF expression in 6-week HBO critical-sized defect samples compared to Room Air samples. Staining of the 12-week HBO samples was reduced compared to 6-week HBO (p=.008) and was similar to 6- and 12-week NBO control samples (Fok et al., 2008), which may indicate earlier effect of HBO therapy on neoangiogenesis and explain the subsequent effect on bone mineral content reduction at that time point.

The critical-sized defect wound is a hypoxic wound. Blood supply to the cranium is primarily through the pericranium and from the dura. It seems that HBO has induced neoangiogenesis through intermittent hypoxia and hyperoxia.

HBO has been shown to stimulate stem cell mobilization from the bone marrow and improve cell growth differentiation (Thom et al., 2006). The significant decrease in bone marrow in HBO Non-Grafted defect may be explained by liberation of all bone marrow pluripotent stem cells to differentiate into osteoblast and obliterate bone marrow spaces. Interestingly, bone marrow decrease in the HBO Grafted defects was not significant compared to NBO Grafted defects, which may be explained by increased bone resorption or angiogenesis.

In vivo studies also demonstrated higher levels of vascular endothelial cell factors expression in stem cells exposed to HBO especially in the presence of lactate (Milovanova et al., 2009). HBO has also been shown to significantly increase the secretion of basic fibroblast growth factor (bFGF) suggesting that daily HBO treatment enhances the fibroblast growth (Kang et al., 2004). We can postulate that HBO has stimulated stem cell mobilization from the edges of the defects to grow and differentiate toward the center, forming bone in place of the fibrous band of tissue that has formed in

NBO Non-Grafted defects. HBO was also shown also to stimulate osteoblast differentiation and activity (Wu et al., 2007). HBO has provided enough oxygen tension for the differentiation of stem cells into osteoprogenitor cells and osteoblasts rather than fibroblasts.

Sawai et al. investigated the effect of HBO on mandibular defect healing with autogenous bone grafts in rabbits by histology. They reported that HBO increased the amount of bone formed initially and that the graft became incorporated into the surrounding bone making it difficult to distinguish the graft from new bone after 4 weeks (Sawai et al., 1996). However, quantitative effects were not evaluated in the aforementioned study. Chen et al. demonstrated that HBO increased the rate of union of rabbit spinal fusions in the presence of autogenous grafts (Chen et al., 2002).

Limitations of this study include a limited sample size. Five animals per group provides total of 10 defects per group. The standard deviation of new bone formation in HBO treated nongrafted defects is measured to be 25.4. The estimated statistical power would be 0.28. Ideally, the statistical power is considered high at 0.8 to 0.9. On the other hand, HBO therapy is time consuming and labor intensive, demanding full time manpower. Administering the HBO protocol for 5 animals is a full time job for at least one month. No more than 5 animals can be treated a day. HBO administration in this study took place over 6 months. The ideal sample size to detect significant differences between HBO and control at a power of 0.8 would be at least 34 defects. This means at least 16 animals per group keeping in mind that each animal would have two calvarial defects.

Chapter VI: Conclusions

HBO treatment sessions as in the protocol described in this study significantly enhanced bone formation within the critical-sized defects, even in the absence of an autograft or a bone substitute. HBO induced bony union in both critical sized 15mm and supracritical sized 18mm defects. Hence, HBO increased the acceptable critical size to more than 20%. This may potentially minimize the amount of the bone graft or bone substitute required to permit healing of bony calvarial defects. HBO may have even negated the need for such adjunctive treatments in this animal model.

In an attempt to determine the quality of the bone regenerated in these defects in the absence of autogenous bone grafting, bone mineral content and density were compared with and without hyperbaric oxygen therapy. HBO therapy enhanced bony healing in non-grafted rabbit calvarial critical-sized defects with a bone volume that is comparable with autogenous non-vascularized bone grafting. Clinical and functional capabilities of this bone volume have yet to be examined, possibly through a functionally loaded implant model in critical-sized mandibular defects.

HBO resulted in a reduction of the bone mineral content of the autogenous bone grafted sites. Angiogenesis within the graft may account for the reduction observed during the experimental period of this study. The clinical significance if this reduction in bone mineral density and bone mineral content has yet to be determined. Further studies with higher statistical power and larger sample sizes should be conducted.

Bibliography

ANG, E., BLACK, C., IRISH, J., BROWN, D. H., GULLANE, P., O'SULLIVAN, B. & NELIGAN, P. C. (2003). Reconstructive options in the treatment of osteoradionecrosis of the craniomaxillofacial skeleton. *Br J Plast Surg* **56,** 92-9.

ATTINGER, C. E., HOANG, H., STEINBERG, J., COUCH, K., HUBLEY, K., WINGER, L. & KUGLER, M. (2008). How to make a hospital-based wound center financially viable: the Georgetown University Hospital model. *Gynecol Oncol* **111,** S92-7.

AXHAUSEN, G. (1907). Histologische untersuch ungen uber knochentransplantation am menschen. . *Deutsche Ztschr F chir Leipz* **93,** 388-92.

AXHAUSEN, W. (1956). The osteogenic phases of regeneration of bone, a histological and experimental study. *J Bone Joint Surg* **38,** 593-601.

BROUSSARD, C. L. (2004). Hyperbaric oxygenation and wound healing. *J Vasc Nurs* **22,** 42-8.

BROWN, D. A., EVANS, A. W. & SÀNDOR, G. K. B. (1998). Hyperbaric Oxygen Therapy in the Management of Osteoradionecrosis of the Mandible. *Advances in Otorhinolaryngology* **54,** 14-32.

BUI, Q. C., LEIBER, M., WITHERS, H. R., CORSON, K. & RIJNSOEVER, M. V. E., H. (2004). The efficacy of hyperbaric oxygen therapy in the treatment of radiation-induced late side effects. *Int J Radiation Oncology Biol Phys* **60,** 871-8.

BURCHARDT, H. (1983). The biology of bone graft repair. . *Clin Orthop* **174,** 28-36.

CEI, S., MAIR, B., KANDLER, B., GABRIELE, M., WATZEK, G. & GRUBER, R. (2006). Age-related changes of cell outgrowth from rat calvarial and mandibular bone in vitro. *J Craniomaxillofac Surg* **34,** 387-94.

CHEN, W. J., LAI, P. L., CHANG, C. H., LEE, M. S., CHEN, C. H. & TAI, C. L. (2002). The effect of hyperbaric oxygen therapy on spinal fusion: using the model of posterolateral intertransverse fusion in rabbits. *The Journal of trauma* **52,** 333-8.

CLOKIE, C. M., MOGHADAM, H., JACKSON, M. T. & SÀNDOR, G. K. (2002). Closure of critical size defects with allogeneic and alloplastic bone substitutes. *J Craniofac Surg* **13,** 111-21.

CONCONI, M. T., BAIGUERA, S., GUIDOLIN, D., FURLAN, C., MENTI, A. M., VIGOLO, S., BELLONI, A. S., PARNIGOTTO, P. P. & NUSSDORFER, G. G. (2003). Effects of hyperbaric oxygen on proliferative and apoptotic activities and reactive oxygen species generation in mouse fibroblast 3T3/J2 cell line. *J Investig Med* **51,** 227-32.

DAVID, L. A., SÀNDOR, G. K. B., EVANS, A. W. & BROWN, D. H. (2001). Hyperbaric oxygen therapy and mandibular osteoradionecrosis: a retrospective study and analysis of treatment outcomes. . *Journal of the Canadian Dental Association* **67,** 384-6.

FELDMEIER, J. J. (2003). Hyperbaric Oxygen 2003-Indications and Results, . *The Hyperbaric Oxygen Committee Report, UHMS*.

FENTON, C. F., KERTESZ, T., BAKER, G. & SÀNDOR, G. K. B. (2004). Necrotising fasciitis of the face: A rare but significant clinical condition *Journal of the Canadian Dental Association* **70,** 604-608.

FOK, T. C., JAN, A., PEEL, S. A., EVANS, A. W., CLOKIE, C. M. & SÀNDOR, G. K. (2008). Hyperbaric oxygen results in increased vascular endothelial growth factor (VEGF) protein expression in rabbit calvarial critical-sized defects. *Oral surgery, oral medicine, oral pathology, oral radiology, and endodontics* **105,** 417-22.

GELFAND, R., LAMBERTSEN, C. J. & CLARK, J. M. (2006). Ventilatory effects of prolonged hyperoxia at pressures of 1.5-3.0 ATA. *Aviat Space Environ Med* **77,** 801-10.

GOLDWASER, B. R., CHUANG, S. K., KABAN, L. B. & AUGUST, M. (2007). Risk factor assessment for the development of osteoradionecrosis. *J Oral Maxillofac Surg* **65,** 2311-6.

GRAY, J. C. & ELVES, M. (1979). Early osteogenesis in compact bone. *Tiss Int* **29,** 225-9.

GRAY, J. C., PHIL, M. & ELVES, M. (1982). Donor cell contribution to osteogenesis in experimental cancellous bone graft. *Clin Orthop* **163,** 261-5.

HADDAD, A. J., PEEL, S. A., CLOKIE, C. M. & SÁNDOR, G. K. (2006). Closure of rabbit calvarial critical-sized defects using protective composite allogeneic and alloplastic bone substitutes. *J Craniofac Surg* **17,** 926-34.

HAM, A. & GORDON, S. (1952). The origin of bone that forms in association with cancellous chips transplanted into muscle. *Br J Plast Surg* **5,** 154-9.

HENDRICKS, P. L., HALL, D. A., HUNTER, W. L. J. & HALEY, P. J. (1977). Extension of pulmonary O2 tolerance in man at 2 ATA by intermittent O2 exposure. *J Appl Physiol* **42,** 593-9.

HOLLINGER, J. O., BUCK, D. C. & SCHMITZ. (1994). Quantitative light microscopy. A powerful tool to assess bone. *Clinics Plastic Surg* **21,** 463-75.

HOLLINGER, J. O. & KLEINSCHMIDT, J. C. (1990). The critical size defect as an experimental model to test bone repair materials. *J Craniofac Surg* **1,** 61-8.

HUNT, T. K., ELLISON, E. C. & SEN, C. K. (2004). Oxygen: at the foundation of wound healing--introduction. *World journal of surgery* **28,** 291-3.

JISANDER, S., GRENTHE, B. & SALEMARK, L. (1999). Treatment of mandibular osteoradionecrosis by cancellous bone grafting. *J Oral Maxillofac Surg* **57,** 936-42.

JOHNSON, P. (1997). Osteoradionecrosis of the jaws: a retrospective study of the background factors and treatment in 104 cases. *J Oral Maxillofac Surg* **55,** 545-6.

KAINULAINEN, V. T., SÁNDOR, G. K., CARMICHAEL, R. P. & OIKARINEN, K. S. (2005). Safety of zygomatic bone harvesting: a prospective study of 32 consecutive patients with simultaneous zygomatic bone grafting and 1-stage implant placement. *The International journal of oral & maxillofacial implants* **20,** 245-52.

KANG, T. S., GORTI, G. K., QUAN, S. Y., HO, M. & KOCH, R. J. (2004). Effect of hyperbaric oxygen on the growth factor profile of fibroblasts. *Arch Facial Plast Surg* **6,** 31-5.

KELLER, E. E., TOLMAN, D. E., ZUCK, S. L. & ECKERT, S. E. (1997). Mandibular endosseous implants and autogenous bone grafting in irradiated tissue: a 10-year retrospective study. *Int J Oral Maxillofac Implants* **12,** 800-13.

LARSON, A., ENGSTROM, M., UUSIJAVRI, J., KIHLSTROM, L., LIND, F. & MATHIESEN, T. (2002). Hyperbaric oxygen treatment of postoperative neurosurgical infections. *Neurosurgery* **50,** 287-95.

MAINOUS, E. G. (1982). Osteogenesis enhancement utilizing hyperbaric oxygen therapy. *Hyperbaric Oxygen Rev* **3,** 181-5.

MARX, R. E. (1984). Osteonecrosis of jaws: review and update. *Hyperbaric Oxygen Rev* **5,** 78-128.

MARX, R. E. (1993). Mandibular reconstruction. *J Oral Maxillofac Surg* **51,** 466-79.

MARX, R. E. (2005). Bone harvest from the posterior ilium. *Atlas Oral Maxillofac Surg Clin North Am* **13,** 109-18.

MARX, R. E., EHLER, W. J., TAYAPONGSAK, P. & PIERCE, L. W. (1990). Relationship of oxygen dose to angiogenesis induction in irradiated tissue. *American journal of surgery* **160,** 519-24.

MARX, R. E., JOHNSON, R. P. & KLINE, S. N. (1985). Prevention of osteoradionecrosis: A randomized prospective clinical trial of hyperbaric oxygen versus penicillin. *J Am Dent Assoc* **11,** 49-54.

MILOVANOVA, T. N., BHOPALE, V. M., SOROKINA, E. M., MOORE, J. S., HUNT, T. K., HAUER-JENSEN, M., VELAZQUEZ, O. C. & THOM, S. R. (2009). Hyperbaric oxygen stimulates vasculogenic stem cell growth and differentiation in vivo. *J Appl Physiol* **106,** 711-28.

MOGHADAM, H. G., SÀNDOR, G. K., HOLMES, H. I. & CLOKIE, C. (2004). Histomorphometric evaluation of bone regeneration using allogeneic and alloplastic bone substitutes. *J Oral Maxillofac Surg* **62,** 202-13.

MUHONEN, A., HAAPARANTA, M., GRONROOS, T., BERGMAN, J., KNUUTI, J., HINKKA, S. & HAPPONEN, R.-P. (2004). Osteoblastic activity and neoangiogenesis in distracted bone of irradiated rabbit mandible with or without hyperbaric oxygen treatment. *Int J Oral Maxillofac Surg* **33,** 173-8.

MUHONEN, A., MUHONEN, J., LINDHOLM, T. C., MINN, H., KLOSSNER, J., KULMALA, J. & HAPPONEN, R.-P. (2002a). Osteodistraction of a previously irradiated mandible with or without adjunctive hyperbaric oxygenation: An experimental study in rabbits. *Int J Oral Maxillofac Surg* **31,** 519-24.

MUHONEN, A., PELTOMAKI, T., HINKKA, S. & HAPPONEN, R. P. (2002b). Effects of mandibular distraction osteogenesis on temporomandibular joint after previous irradiation and hyperbaric oxygenation. *Int J Oral Maxillofac Surg* **31,** 379-404.

MUHONEN, A., PELTOMAKI, T., KNUUTI, J., RAITAKARI, O. & HAPPONEN, R. (2002c). Osteoblastic activity of the rabbit temporomandibular joint during distraction osteogenesis assessed by [18F] fluoride positron emission tomography. *Eur J Oral Sc* **110 Apr,** 144-8.

NILSSON, L. P. (1989). Effects of hyperbaric oxygen treatment on bone healing. An experimental study in the rat mandible and the rabbit tibia. *Swedish dental journal* **64,** 1-33.

NILSSON, P., ALBERKTSSON, T., GRANSTROM, G. & ROCKERT, H. O. (1988). The effects of hyperbaric oxygen treatment on bone regeneration: An experimental study using bone harvest chamber in the rabbit. *Int J Oral Maxillofac Impl* **3,** 43-8.

OZERDEM, O. R., ANLATICI, R., BAHAR, T., KAYASELCUK, F., BARUTCU, O., TUNCER, I. & SEN, O. (2003). Roles of periosteum, dura, and adjacent bone on healing of cranionecrosis. *J Craniofac Surg* **14,** 371-9.

PARFITT, A. M. (1976). The actions of parathyroid hormone on bone: relation to bone remodeling and turnover, calcium homeostasis, and metabolic bone disease. Part I of IV parts: mechanisms of calcium transfer between blood and bone and their cellular basis: morphological and kinetic approaches to bone turnover. *Metabolism* **25,** 809-44.

SAWAI, T., NIIMI, A., TAKAHASHI, H. & UEDA, M. (1996). Histologic study of the effect of hyperbaric oxygen therapy on autogenous free bone grafts. *J Oral Maxillofac Surg* **54 Aug,** 975-81.

SCHENK, R. K. & WILLENEGGER, H. R. (1977). Histology of primary bone healing: modifications and limits of recovery of gaps in relation to extent of the defect. *Unfallheilkunde* **5,** 155-60.

SCHMITZ, J. P. & HOLLINGER, J. O. (1986). The critical size defect as an experimental model for craniomandibulofacial nonunions. *Clin Orthop Relat Res* **205,** 299-308.

SEVERINGHAUS, J. W. (2003). Fire-air and dephlogistication. Revisionisms of oxygen's discovery. *Adv Exp Med Biol* **19,** 543:7.

SHEIKH, A. Y., ROLLINS, M. D., HOPF, H. W. & HUNT, T. K. (2005). Hyperoxia improves microvascular perfusion in a murine wound model. *Wound Repair Regen* **13,** 303-8.

SHIRELY, P. & ROSS, J. (2001). Hyperbaric medicine part 1: theory and practice. *Current Anaesthesia & Critical Care* **12,** 114-20.

TANDARA, A. A. & MUSTOE, T. A. (2004). Oxygen in wound healing--more than a nutrient. *World journal of surgery* **28,** 294-300.

THOM, S. R., BHOPALE, V. M., VELAZQUEZ, O. C., GOLDSTEIN, L. J., THOM, L. H. & BUERK, D. G. (2006). Stem cell mobilization by hyperbaric oxygen. *Am J Physiol Heart Circ Physiol* **290,** H1378-86.

TUNCAY, O. C., HO, D. & BARBER, M. K. (1994). Oxygen tension regulates osteoblast function. *Am J Orthod Dentofacial Orthop* **105,** 457-63.

VAN GOLDE, J. M., MULDER, T. A., SCHEVE, E., PRINZEN, F. W. & BLANCO, C. E. (1999). Hyperoxia and local organ blood flow in the developing chick embryo. *J Physiol* **515,** 243-8.

WAGNER, W., ESSER, E. & OSTKAMP, K. (1998). Osseointegration of dental implants in patients with and without radiotherapy. *Acta Oncol* **37,** 693-6.

WU, D., MALDA, J., CRAWFORD, R. & XIAO, Y. (2007). Effects of hyperbaric oxygen on proliferation and differentiation of osteoblasts from human alveolar bone. *Connect Tissue Res* **48,** 206-13.